

**Fleet-based vehicle emission factors using low-cost sensors:
Methodology development and validation**

by

Bingqi Liu

B.Eng., Jilin University, 2018

A THESIS SUBMITTED IN PARTIAL FULFILLMENT OF
THE REQUIREMENTS FOR THE DEGREE OF

MASTER OF APPLIED SCIENCE

in

THE FACULTY OF GRADUATE AND POSTDOCTORAL STUDIES
(Mechanical Engineering)

THE UNIVERSITY OF BRITISH COLUMBIA
(Vancouver)

August 2020

© Bingqi Liu, 2020

The following individuals certify that they have read, and recommend to the Faculty of Graduate and Postdoctoral Studies for acceptance, a thesis entitled:

Fleet-based vehicle emission factors using low-cost sensors: Development and validation of methodologies

submitted by Bingqi Liu in partial fulfillment of the requirements for
the degree of Master of Applied Science
in Mechanical Engineering

Examining Committee:

Dr. Naomi Zimmerman, Assistant Professor, Mechanical Engineering, UBC
Supervisor

Dr. Amanda Giang, Assistant Professor, Mechanical Engineering and IRES, UBC
Supervisory Committee Member

Dr. Patrick Kirchen, Associate Professor, Mechanical Engineering, UBC
Supervisory Committee Member

Abstract

Traditionally, vehicle emissions measurements have relied on reference-grade instruments whose high cost and complexity have limited their deployment in real-world environments. New simple-to-operate, low-cost sensing technologies are a potential solution to this problem. This work aims to validate whether low-cost sensors, with proper calibration, could measure vehicle emissions and could support analysis of emission trends. Under that umbrella, this work provides a comprehensive low-cost solution to the measurement of vehicle emissions factors within the vehicle fleet. The Sensit Real-time, Affordable, Multi-Pollutant (RAMP) monitors measuring $PM_{2.5}$, NO, NO_2 , CO_2 , O_3 , and CO were the low-cost sensor used. The RAMPs were first calibrated based on a collocation with a near-road regulatory site. To assess their suitability of measuring vehicle emissions, six RAMPs were deployed in three parking garages on the UBC Vancouver campus from April–August 2019. UBC Parking Services provided real-time vehicle counts to help validate our method. After sensor calibration, integrated pollutant and CO_2 signals were converted to fuel-based emission factors (EFs) by developing a background subtraction and plume identification algorithm. The calculated EFs fell within the range of previous studies. Evening-vehicle leaving EFs when vehicles were cold were 10-50% higher than in the morning. We also observed a disproportional contribution of high emitters; the top 25% of plumes contributed 45-65% of total emissions. The findings indicate that low-cost sensors are a promising technology for real-world vehicle emissions measurement.

Lay Summary

Recently, the development of low-cost sensing technologies has made widespread real-world pollution monitoring possible. This thesis explores how low-cost air pollution sensing can be applied to vehicle emissions measurement. As part of this exploration, a detailed calibration protocol was developed, and the sensors were piloted across parking garages on the UBC Vancouver campus. Based on a comparison of the data to published studies, low-cost sensors are a promising tool for the real-world measurement of vehicle emissions.

Preface

This thesis is based on a research project supervised by Dr. Naomi Zimmerman. The idea for this project was originally developed by Dr. Naomi Zimmerman and the experiments were designed by Dr. Naomi Zimmerman with input from M.A.Sc student Bingqi Liu. M.A.Sc student Bingqi Liu conducted the entirety of the measurement campaign on the UBC Vancouver campus, with support from UBC Parking Services for sensor installation. M.A.Sc student Bingqi Liu conducted the sensor calibration analysis, with support from Ph.D. candidate Mrinmoy Chakraborty and Ph.D. candidate Sakshi Jain to help move and install the sensors at the calibration site. Bingqi Liu conducted all data analysis work within this project.

A combined and shortened version of Chapters 3-5 was submitted as:

Liu, B., Zimmerman, N., 2020. "Fleet-based vehicle emission factors using low-cost sensors: Case study in parking garages" *Transportation Research Part D, Transport and Environment*.

The author of this thesis was the principal contributor to this work.

Table of Contents

Abstract.....	iii
Lay Summary	iv
Preface.....	v
Table of Contents	vi
List of Tables	x
List of Figures.....	xi
List of Abbreviations	xiv
Acknowledgements	xvi
Chapter 1: Introduction	1
1.1 Motivation: Air Pollution from Transportation	1
1.2 Testing of Vehicle Emissions	2
1.3 New tools: Low-cost Sensors.....	3
1.4 Objectives and Outline.....	3
1.4.1 Thesis Outline	4
Chapter 2: Literature Review.....	5
2.1 Introduction.....	5
2.2 Vehicle Emissions and Health Impacts.....	5
2.3 Emissions Regulations	7
2.4 Emissions Measurement Techniques	9
2.4.1 Laboratory-Based Measurement.....	9
2.4.2 Real-world Based Measurement	11

2.5	Emissions Reduction Strategies	15
2.5.1	After-treatment.....	15
2.5.2	Other approaches	16
2.6	Low-cost air pollution sensors	16
2.6.1	Characteristics of low-cost sensors.....	16
2.6.2	Calibration techniques	18
2.7	Conclusions.....	21
Chapter 3: Instrumentation and Calibration.....		23
3.1	Introduction.....	23
3.2	Real-time Affordable Multi-Pollutant Monitor	24
3.3	Sensor Calibration.....	26
3.3.1	Collocation Campaign	26
3.3.2	Calibration of Gas Sensors.....	29
3.3.2.1	Random forest (RF) model	29
3.3.2.2	Hybrid model	29
3.3.3	Calibration of PM _{2.5} Sensor	34
3.4	Conclusions.....	37
Chapter 4: Development of Vehicle Fleet Emission Factors in Parkades		38
4.1	Introduction.....	38
4.2	Measurement Sites	38
4.2.1	Physical Features of Sampling Locations	38
4.2.2	Traffic Patterns at the Sites	40
4.3	Data processing.....	41

4.3.1	Background Subtraction.....	41
4.3.2	Fuel-based Emission Factors	45
4.3.3	Determination of Vehicle Emissions Detection Limit.....	48
4.3.4	Plume Identifying and Matching	48
4.4	Results and Discussion	49
4.4.1	Diurnal Pollutant Patterns	49
4.4.2	Overall Fleet-based Emission Factors	51
4.4.3	Determination of the Relative Importance of Cold Start	53
4.4.4	Assessing the relative contribution of high emitters.....	57
4.5	Errors and uncertainty.....	59
4.5.1	Uncertainty of the instruments.....	59
4.5.2	Uncertainty of the methods.....	60
4.6	Conclusions.....	60
Chapter 5: Conclusions and Future work		62
5.1	Overall Conclusions.....	62
5.2	Revisiting the Objectives	63
5.2.1	Objective 1: Calibrating low-cost sensors in a traffic-rich environment.....	63
5.2.2	Objective 2: Developing a method for determining fleet-based vehicle emission factors with low-cost sensor data.....	63
5.2.3	Objective 3: Comparing the calculated emission factors to those in the published literature	63
5.2.4	Objective 4: Assessing the relative importance of cold start on vehicle emissions.	64
5.3	Limitations of This Work and Challenges of the Field.....	64

5.3.1	The limitation of our study exists in several aspects	64
5.3.2	Challenges in the field more broadly	65
5.4	Implications for stakeholders and future research directions	67
5.4.1	Implications for stakeholders	67
5.4.2	Future research directions	68
Bibliography		70
Appendices.....		90
Appendix A.....		90
A.1	Plume detection and matching details.....	90
A.2	Diurnal trend of hourly average pollutant concentrations before and after background subtraction.....	92

List of Tables

Table 2.1 Past and current emissions standards for light-duty vehicles in the United States and Europe.	8
Table 2.2 Comparison of different emissions monitoring approaches.	13
Table 3.1 Configurations of the sensors inside the RAMP monitor.	24
Table 3.2 Configurations of the sensors at Clark Drive site.	27
Table 3.3 Comparison of Calibration Results between our attempt and the original results published by Zimmerman et al. (2018) and Malings et al. (2019).	34
Table 3.4 Comparison of PM _{2.5} Calibration Result between our attempt and the original results published by Malings et al. (2020).	36
Table 4.1 Characteristics of the parking garages.	39
Table 4.2 Comparing the average emission factors developed in this study with previous work (light-duty vehicles only). To convert fuel-based emission factors into distance-based emission factors, we used an average fuel economy of 9L/100 km and a fuel density of 0.755 kg/L. Our EFs are expressed as average +/- a 95% confidence interval (The emission factors developed from Site BG1 center were not included) and the uncertainty of the instruments after calibration is not included.	52
Table A.1 Pollutant cut-off values at the different measurement sites to determine our plume threshold.	90
Table A.2 Number of matched pollutant-CO ₂ plumes for emission factor calculations.	91

List of Figures

Figure 2.1 The United States Federal Test Procedure (FTP-75), an example drive cycle used to assess vehicle emissions compliance with regulatory standards.	9
Figure 3.1 RAMP mounted in a parking garage (right) and the bottom of a RAMP monitor showing the location of the sampling units (left).....	25
Figure 3.2 Picture inside the weather-proof shell of the RAMP, each low-cost sensor is marked with the target it measures. The sensors inside this package are independent of each other and could be replaced quickly when damaged.	25
Figure 3.3 Picture of the collocation site at Clark Drive in Vancouver, BC beside a major roadway the sensors are deployed close to (within 2 meters) the sampling pipe of reference-grade instruments. The primary monitoring target of this site is the emissions from vehicles passing by.	28
Figure 3.4 Determination of the cut-off point for switching from the random forest model to the MLR model based on changes to r^2 . In this case, the r^2 is approaching the greatest value when the upper percentage limit for the RF model is around 98%, thus 98% is selected.	32
Figure 3.5 Performance of the calibration models on the withheld testing data for the gas sensors of all of the RAMPs in this study. CvMAE is the coefficient of variation of the mean absolute error (i.e., the mean absolute error normalized by the average concentration). CvMAE can be interpreted as the approximate percent error (e.g., ~ 15% for ozone). For the box plots, whiskers are 10 th and 90 th percentile, box edges are 25 th and 75 th percentiles, and the line is the median..	33
Figure 3.6 Performance of the calibration models on the withheld testing data for the PM _{2.5} sensors of all of the RAMPs in this study. CvMAE is the coefficient of variation of the mean	

absolute error (i.e., the mean absolute error normalized by the average concentration). CvMAE can be interpreted as an approximate percent error. For the box plots, whiskers are 10th and 90th percentile, box edges are 25th and 75th percentiles, and the line is the median..... 36

Figure 4.1 Schematic of the parking garages and relative positions of RAMPs, see Table 4.1 for details. The white hexagons represent the RAMP measurement locations. The dash outlines and solid outlines represent an open structure and closed structure, respectively. The angled walls on the top and bottom of AG1 represent the Venetian blind walls on the exterior of the garage. All of the RAMPs are on the same floor except for the RAMPs in Site AG2 in which the RAMP in the center is on the second floor and the distance between the sensors on the same Site is around 50m. 40

Figure 4.2 Hourly average vehicle counts at the three parking garages in this study..... 41

Figure 4.3 Average Stability and Adherence parameters across all campaign days for CO at Site AG2 as a function of window length. 44

Figure 4.4 The influence of window width and smoothing index on the background concentrations. This is an example of the monitoring data from Site AG2 for around 24 hours. 45

Figure 4.5 Flowchart for identifying start and end times of pollutant and CO₂ plumes. Here [x,y] is the start and end time of a pollutant plume and [a,b] is the start and end time of the CO₂ plume. If plume peaks and local minimums meet specific criteria based on the emissions cut off, and the pollutant and CO₂ plumes are within 2 data points of each other, then an emission factor is calculated. 49

Figure 4.6 Diurnal trend of the hourly average concentrations of targeted gases in Site AG2. The orange curves represent the measurement spot inside the Site AG2, and the blue curves represent the measurement spot at the gate of Site AG2..... 50

Figure 4.7 Comparison of Emission factors (1: CO; 2: NO_x) between morning entering vehicles and evening leaving vehicles from 6 measurement spots of 3 sites. For the box plots, whiskers are 10th and 90th percentile, box edges are 25th and 75th percentiles, the line is the median, and the circle markers in blue are the average..... 54

Figure 4.8 Relative contribution of heavy emitters. Side 1 shows the morning entering EFs, and Side 2 shows both morning entering and evening leaving EFs (excluding site BG1 center). 58

Figure A.1 Diurnal trends of hourly average pollutant total concentrations. The orange curve is the concentration at the center of the garage and the blue curve is the concentration at the gate of the garage. 92

Figure A.2 Diurnal trends of hourly average background-subtracted concentrations. The orange curve is the concentration at the center of the garage and the blue curve is the concentration at the gate of the garage. 93

List of Abbreviations

AG:	Above ground parking garage
BC:	Below ground parking garage
CO:	Carbon monoxide
CO ₂ :	Carbon dioxide
CvMAE:	Coefficient of variation of the mean absolute error
DP:	Dew point
EF:	Emission factor
EGR:	Exhaust gas recirculation
FTP:	(US) Federal test procedure
GDI:	Gasoline direct injection
HC:	Hydrocarbon
HDV:	Heavy-duty vehicle
ICE:	Internal combustion engine
LCS:	Low-cost sensor
LDV:	Light-duty vehicle
MLR:	Multiple linear regression
NEDC:	New European driving cycle
NDIR:	Nondispersive infrared
NO:	Nitrogen monoxide
NO _x :	Nitrogen oxides including NO ₂ and NO
NO ₂ :	Nitrogen dioxide

Pearson R:	Pearson coefficient of correlation
PEMS:	Portable emissions measurement system
PM:	Particle matter
PM _{2.5} :	Particle matter equal to or less than 2.5 µm in aerodynamic diameter
RAMP monitor:	Real-time Affordable Multi-Pollutant monitor
RF:	Random forest
RGI:	Reference-grade instrument
RH:	Relative humidity
SCR:	Selective catalytic reduction
SO ₂ :	Sulfur dioxides
T:	Temperature
TWC:	Three-way catalyst
UBC:	University of British Columbia
WLTC:	Worldwide harmonized light vehicles test procedure

Acknowledgements

Firstly, I would like to thank my supervisor, Professor Naomi Zimmerman, for her trust, patience, expectations, and financial support during my studies at UBC. Looking back to the beginning of graduate school, I know my progress would have not been possible without her guidance and support. Her exceptional supervision not only made me a better researcher, but also a better person. She has been working as my role model over the past 2 years. I'm especially glad to be her first student to onboard as well as to complete.

I would also like to thank Prof. Amanda Giang and Prof. Patrick Kirchen for serving as my committee members and giving valuable feedback on my research work. Also, I want to thank Prof. Steven Rogak for introducing me to UBC, offering me a teaching assistantship, and providing me and the iREACH team with great help.

I would like to thank my fellow graduate students, Sakshi, Melanie, and Mrinmoy for encouragement and friendship. To my friends in Vancouver, Kelowna, Changchun, and Wuhan that have been encouraging me for the past 2 years, I want to say thank you and keep in touch.

This study was supported by NSERC and the Mitacs Globalink Graduate Fellowship program. UBC Parking Services and Metro Vancouver also provided important assistance to my project.

Last but not the least, I would like to thank my parents for their unconditional love and support.

Chapter 1: Introduction

1.1 Motivation: Air Pollution from Transportation

According to the World Health Organization, air pollution is a leading cause of premature mortality and is associated with over 7 million deaths per year (Campbell-Lendrum and Prüss-Ustün, 2019; Dedoussi et al., 2020; Health Canada, 2016; Lelieveld et al., 2015; Wong, 2014). Among air pollution sources, the transportation sector is a large contributor; in North America, the transportation sector accounted for approximately 20% of total PM_{2.5} pollution in recent years (Anenberg et al., 2019; Meng et al., 2019). Furthermore, in 2019 almost a third of all fossil fuel consumption in the US was from the transportation sector, underscoring the critical role of transportation emissions monitoring and management as part of climate change abatement (U.S. Department of Energy, 2020). The majority of the emissions from the transportation sector are emitted by internal combustion engines (ICEs) (York and Rouleau, 2017). ICE vehicles have variable emissions rates due to numerous factors such as operating and environmental conditions, fuels, vehicle type, and after-treatment devices. Among the different working phases of an ICE engine, the cold start phase has a disproportionately high emission rate due to poorer combustion efficiency at lower temperatures, a lower air-to-fuel ratio, and reduced conversion efficiency of the after-treatment devices (such as the three-way-catalyst in gasoline engines which converts the NO_x, CO and hydrocarbons into non-toxic components of air) below light-off temperature. The disproportional contribution of emissions during the cold start phase has been found by both in-lab (up to 34% of NO_x in the drive cycle) and on-road studies (more than 50% of CO in the driving route) (Johnson and Joshi, 2017; Khan and Frey, 2018; Singer et al., 1999).

1.2 Testing of Vehicle Emissions

To limit the negative impacts of engine emissions and improve urban air quality, emissions regulations have been put forward and progressively tightened since the 1960s (Franco et al., 2013; Gerard and Lave, 2005; Johnson and Joshi, 2017; Kumar Pathak et al., 2016; Ropkins et al., 2017; Tietge et al., 2015a). Along with adjustments to vehicle emission regulations, emissions measurement procedures and technologies have also been evolving to better assess the factors affecting vehicle emission rates. The bulk of this evolution has been in the calculation of vehicle emission factors (EFs), which normalize emissions to the activity that causes them (e.g., emissions per distance travelled or per kg fuel burned) (Huang et al., 2018; Johnson and Joshi, 2017; Wang et al., 2018a). An EF can be calculated using either laboratory-based testing or real-world measurement (either near-road or on-road). In laboratory testing, vehicle or engine exhaust is sampled directly from the exhaust pipe and EFs are calculated for the specific engine or vehicle being tested (Franco et al., 2013; Johnson and Joshi, 2017). Real-world EFs can be separated into approaches that measure the fleet average, such as remote sensing and tunnel studies, and approaches for measuring individual vehicles, such as chase measurements or portable emissions monitoring systems (PEMS) (Franco et al., 2013; Huang et al., 2018; Wang et al., 2015; Zimmerman et al., 2016). The laboratory-based measurements have the advantage of precision and a detailed breakdown by operating condition; however, these measurements are expensive and only a limited number of vehicles can be tested. Furthermore, although transient operating phases are included in laboratory-based measurements, the driving cycles do not fully reflect real-world driving conditions due to meteorology conditions, external traffic conditions and unpredictable driving behaviours (Zimmerman, 2016). Real-world approaches can be used to assess far more vehicles, particularly when using remote sensing/near-road plume-based monitoring, however, the

EFs are only representative of the driving conditions encountered at the specific sampling location, and the uncertainty is increased (Huang et al., 2018; Wang et al., 2015; Zimmerman et al., 2016).

1.3 New tools: Low-cost Sensors

To date, high-cost regulatory-grade instruments have been the primary tool for assessing real-world and laboratory-based EFs. These instruments are well-designed with rigid quality assurance standards and a narrow range of signal uncertainty. Recently, low-cost sensors (LCSs) have been increasingly used in ambient air quality studies, with a focus on demonstrating their accuracy using different calibration approaches (Castell et al., 2017; Jiao et al., 2016; Malings et al., 2020; Zimmerman et al., 2018). The operation of LCS systems is far less complex than traditional instruments and these tools are typically small and portable, creating the potential for widespread deployment in urban areas where traffic-related pollution is substantial. One potential application of widespread LCS deployment is using LCS systems as a remote sensing tool for the measurement of fleet-based EFs. If these tools could be used for this purpose, LCS systems could be deployed at hundreds of locations to capture a broad range of vehicle operating conditions and environments, generating millions of vehicle plumes for analysis. However, it remains uncertain if the measurement sensitivity of LCS systems is capable of such measurements.

1.4 Objectives and Outline

The overarching objective of this thesis is to assess the suitability of LCS systems for determining fleet-based EFs using a remote-sensing-type approach. In this study, we deployed 6 LCS monitors in 3 parking garages on the University of British Columbia (UBC) campus in Vancouver, British Columbia. These traffic-rich environments combined with vehicle counting data provided by UBC

Parking Services enabled us to develop our method with some built-in validation. Four specific sub-objectives included:

1. Calibrating low-cost sensors in a traffic-rich environment
2. Developing a method for determining fleet-based vehicle emission factors with low-cost sensor data
3. Comparing the calculated emission factors to those in the published literature
4. Assessing the relative importance of cold start on vehicle emissions

1.4.1 Thesis Outline

This thesis comprises five chapters. **Chapter 1** of this thesis provides the background for this study and outlines the thesis objectives. **Chapter 2** of this thesis reviews the current literature within the topics of air pollution, vehicle emissions and emissions measurement. This includes a discussion of calibration approaches in the literature for low-cost air pollution monitors. **Chapter 3** of this thesis describes the instrument calibration approach and performance. **Chapter 4** discusses the comprehensive data processing method for converting low-cost sensor data into fleet-based emission factors. The diurnal pollutant concentrations, average emission factors compared to literature, and the estimated impact of cold start emissions are also discussed. In **Chapter 5**, the overarching conclusions from this thesis, limitations of the work, and future directions are discussed.

Chapter 2: Literature Review

2.1 Introduction

In this literature review, the fundamentals of vehicle emissions and their health impacts will be introduced. Subsequently, the regulations surrounding vehicle emissions and the existing and emerging tools for measuring vehicle emissions are identified and evaluated. Lastly, new opportunities for mitigating and measuring vehicle emissions are discussed.

2.2 Vehicle Emissions and Health Impacts

On-road vehicles are a significant source of air pollutants (Fan and Perry, 2018). As such, management of vehicle emissions is a critical issue in the field of air quality (Henneman et al., 2017; Bento et al., 2015; Kelly and Zhu, 2016). Despite vehicles being increasingly powered by renewable fuels (e.g., electricity, natural gas) that are expected to provide us with cleaner mobility (Yuan et al., 2015), vehicles powered by internal combustion engines (ICEs) will remain the dominant transportation technology in the near term (Johnson and Joshi, 2017). The most common ICEs used on vehicles are four-stroke ICEs, which have one combustion per two rotations, generating extremely high temperature and pressure followed by the downwards movement of the piston, completing the energy conversion (Zhao et al., 1999). Vehicles powered by ICEs emit numerous gaseous and particulate substances as a by-product of incomplete combustion. Typically, scientists have classified nitrogen oxides (NO_x), sulfur oxides (SO_x), carbon monoxide (CO), particulate matter (PM), and volatile organic compounds (VOCs) as major air pollutants from vehicles (Johnson and Joshi, 2017; Krecl et al., 2018). Most of these emissions are generated during fuel combustion, while some of the pollutants, such as PM and VOCs can also be emitted by the brake system, evaporative losses or the tire wear (Kukutschová and Filip, 2018; Boere et

al., 2019; Man et al., 2020; Yamada et al., 2018). These pollutants may go on to react in the atmosphere, producing secondary pollutants such as ozone (O₃). Emissions are significantly influenced by operating conditions, such as engine speed and load (Kumar Pathak et al., 2016; Wang et al., 2014; Zhao et al., 1999). For example, studies have shown that low temperatures during engine start-up periods (also referred to as cold start) can substantially increase emissions (Cédric et al., 2016; Reiter and Kockelman, 2016; Start et al., 2014). It has also been shown that NO_x emissions correspond to the acceleration events (Kumar Pathak et al., 2016) and that idling increases emission of particles and multiple gaseous pollutants, especially VOCs (Lin et al., 2015; Zhang et al., 2020; Lee et al., 2018; Deng et al., 2020; Jabali and Laporte, 2016).

Primary and secondary pollutants emitted by vehicles are associated with significant adverse health impacts such as cardiovascular disease and premature mortality (Brauer et al., 2016; Kennedy, 2007; Lelieveld et al., 2015; Pereira et al., 2014; Rice et al., 2016). Furthermore, engine exhaust has been classified as a carcinogen in humans by the International Agency for Research on Cancer based on long-term epidemiological studies (Silverman, 2012; Breuer and Burgard, 2019; Peters et al., 2017; Franco et al., 2013; Taxell and Santonen, 2017). Within the exhaust, the toxicity of gaseous pollutants depends on their chemical properties, but have been shown to cause damage to the respiratory system by inducing inflammation or asphyxia (May et al., 2017; Wu et al., 2016). The health impacts of exposure to vehicle exhaust PM is more complex due to the various sizes, structures, and components of the PM. Due to this uncertainty, PM emissions are generally regulated based on total mass or number concentration of PM below a specific diameter (e.g., limits on mass concentrations of PM with a diameter of 2.5 μm or smaller). Basing regulation on particle diameter is due to research showing that fine particles (diameter <2.5 μm, PM_{2.5}) and

ultra-fine particles (diameter < 100 nm) can enter the blood system through the lung, resulting in cell inflammation and possibly cell death (Alföldy et al., 2009; Creutzenberg, 2012). The health impacts from vehicle exhaust PM exposure can also depend on the composition; exposure to trace metals, such as zinc, lead, and manganese, can cause an acute inflammation response (Kennedy, 2007; Rice et al., 2016).

Traditionally, diesel engines have been the primary source of vehicle PM. However, with the introduction of gasoline direct injection (GDI) engines, gasoline vehicles are becoming a growing source of PM, especially in the ultrafine size range which has greater health impacts (Franco et al., 2013; Zhu et al., 2016).

2.3 Emissions Regulations

As our understanding of the impacts of vehicle emissions has grown, so too have vehicle emissions regulations (Yuan et al., 2015). The United States was the first country to introduce a nationwide air quality act in 1955, the Air Pollution Control Act, which paved the way for the 1963 Clean Air Act and the 1965 Motor Vehicle Exhaust Control Act (Kuklinska et al., 2015; Stern et al., 2012). Currently, two sets of emission standards exist in the United States: the federal standard established by the US Environmental Protection Agency (US EPA), and the often stricter regulations established by the California Air Resources Board (CARB) (Kuklinska et al., 2015). Current US EPA standards (Tier 3) are mostly harmonized with the current CARB LEV III standards, and Canadian emissions standards are harmonized with those set out by the US EPA. These emissions regulations limit the amount of CO, NO_x, total hydrocarbons (THC), non-methane hydrocarbons (NMHC), non-methane organic gases (NMOG), PM, and total particle number (PN) emitted per

unit distance, known as a distance-based emission factor. The United States and European Emissions regulations for light-duty vehicles (LDVs) are outlined in Table 2.1. Compliance with the emissions limits in Table 2.1 is assessed using either laboratory or real-world based emissions testing on specified drive cycles (e.g., FTP-75). This is discussed in Section 2.4. Heavy duty vehicles (HDVs) also contribute to a large portion of the total emissions (especially for NO_x and PM) while accounting for the minority of the on-road fleet (Gertler, 2005; H. Wang et al., 2008) and the emission standards for HDVs are also being enforced in both United States and Europe.

Table 2.1 Past and current emissions standards for light-duty vehicles in the United States and Europe.

		United States			Europe		
		Tier 1 ^a	Tier 2 ^b	Tier 3 ^c	EURO 4 ^d	EURO 5 ^d	EURO 6 ^d
		1994-1997	2004-2009	2017-2025	2005	2009	2014
THC	g/km	--	--	--	0.1	0.1	0.1
NMHC	g/km	0.50	--	--	--	0.068	0.068
NMOG	g/km	--	0.06	--	--	--	--
NO _x + NMOG	g/km	--	--	0.1	--	--	--
NO _x	g/km	0.96	0.04	--	0.08	0.06	0.06
CO	g/km	2.61	2.61	2.61	1.00	1.00	1.00
HCHO	mg/km	--	11.2	2.49	--	--	--
PM	mg/km	--	6.2	1.86 ^e 0.62 ^f	--	4.5	4.5
PN#	#/km	--	--	--	--	--	6E+12 ^g 6E+11 ^h

^a Passenger cars, 100,000 miles / 10 years, FTP-75 drive cycle

^b Light-duty vehicles, Bin 5, 120,000 miles / 10 years, FTP-75 drive cycle

^c Light-duty vehicles, Bin 160, 120,000 miles / 10 years, FTP-75 drive cycle

^d Category M1 vehicles, New European Drive Cycle (NEDC)

^e phased in 2017-2021 (3 mg/mile)

^f phased in 2025-2028 (1 mg/mile)

^g 2014-2017

^h 2017-onwards

2.4 Emissions Measurement Techniques

2.4.1 Laboratory-Based Measurement

As introduced in Section 2.3, compliance with emissions regulations is typically assessed using laboratory-based measurements. During laboratory testing, the engine or entire vehicle is mounted on a dynamometer, run through drive cycles, and exhaust is directly sampled for analysis (Franco et al., 2013; Zhao et al., 1999; Zhu et al., 2016). A drive cycle is a prescribed operating pattern for the engine and is designed to represent different driving behaviours such as cold start, idling, acceleration, and steady-state driving (Franco et al., 2013; Yuan et al., 2015; Zimmerman, 2016).

Example drive cycles include the US Federal Test Procedure (FTP-75, illustrated in Figure 2.1), the New Europe Driving Cycle (NEDC), which is used in Europe, and the Worldwide Harmonized Light Vehicles Test Procedure (WLTC), which is replacing the NEDC.

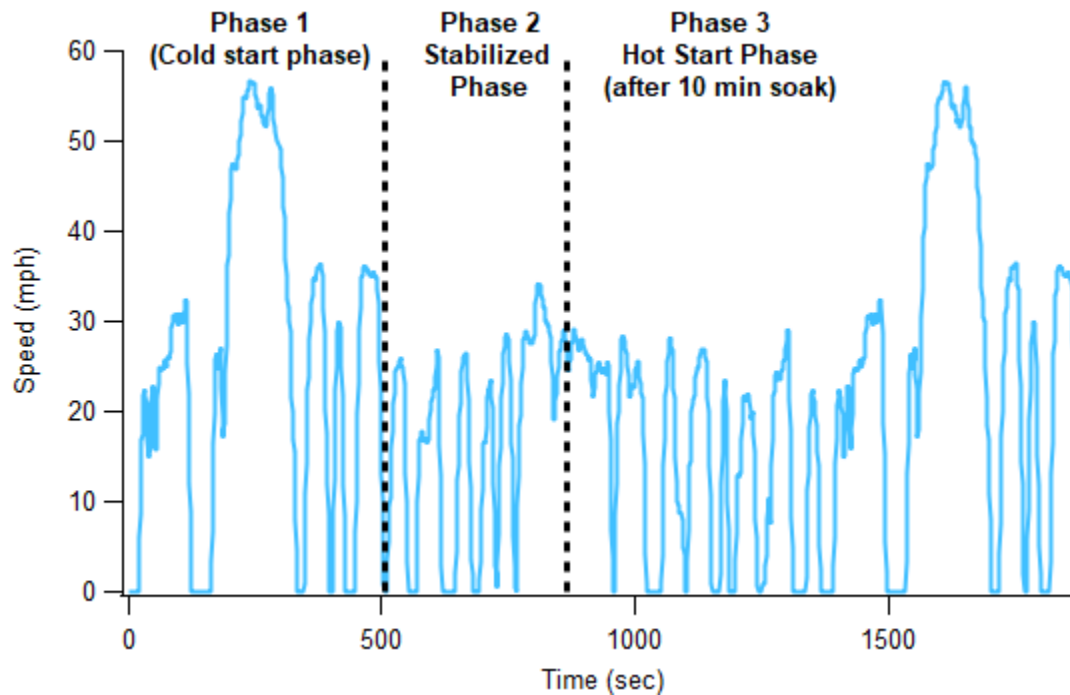


Figure 2.1 The United States Federal Test Procedure (FTP-75), an example drive cycle used to assess vehicle emissions compliance with regulatory standards.

Even though the regulatory laboratory-based drive cycles assess vehicle emissions during dynamic operation across a wide operating range, some studies have identified discrepancies between drive-cycle-based emission rates and emission rates measured in real-world environments (Chang et al., 2018; Pathak et al., 2016). For example, numerous studies have shown that the fuel economy (and subsequent CO₂ emissions) as reported by engine manufacturers are difficult to replicate in real-world contexts (Franco et al., 2013; Tietge et al., 2015). Ramos et al. (2018) also found that engine parameters, such as fuel injection quantity or exhaust gas recirculation valve position, were different between laboratory testing using the NEDC and on-road testing using the newly developed European Real-Driving Emissions test; NO_x emissions were also higher during real-driving operation. Similarly, Degraeuwe and Weiss. (2017) raised concern about the current certification procedure yielding lower emissions than what is observed in the real-world. In real-world conditions, higher emission rates have been observed at traffic intersections when vehicles accelerate or turn (Lin et al., 2015; Qiao et al., 2005). In addition to discrepancies between laboratory-based testing and real-world emissions, choice of drive cycle will also affect emissions. The different speed and acceleration profiles in the NEDC and WLTC cycles have been shown to result in different CO₂ emissions estimates (Ko et al., 2017). Bielaczyc et al. (2020) also compared emissions under FTP-75, NEDC and WLTC and identified systematic differences. Finally, secondary pollutants are generally not measured using laboratory-based drive cycle tests. In some cases, the secondary PM may account for the majority of the PM emitted from vehicles, as such laboratory-based tests may underestimate the true emissions impacts (Kennedy, 2007).

2.4.2 Real-world Based Measurement

As introduced in Section 2.4.1, laboratory-based testing may not reflect the air quality impacts vehicles in the real-world. For example, in Khan and Frey. (2018), a large gap was found between laboratory-based testing and on-road real-world testing, with the real-world test showing substantially higher emissions. Real-world emissions are affected by meteorological conditions, external traffic conditions and unpredictable driving behaviours. Furthermore, primary pollutants may have subsequent reactions after being released into the air resulting in the production of secondary pollutants, which should ideally be considered while assessing vehicle emissions (Gong et al., 2018; Huang et al., 2018; Johnson and Joshi, 2017b; Kumar Pathak et al., 2016; Wang et al., 2008).

To address this issue, there has been increasing interest in assessing vehicle emissions in the real-world to increase the representativeness of the measurements (Huang et al., 2018; Khan and Frey, 2018), while also acknowledging that real-world tests are not as repeatable as laboratory tests (Johnson and Joshi, 2017). Different real-world measurement methods have different advantages and drawbacks. The real-world measurement method closest to that measured in the laboratory is the portable emissions monitoring system (PEMS). A PEMS samples directly from the tailpipe during real-world vehicle operation. As such, the PEMS method takes the different driving behaviour and can provide emissions measurements on an individual-vehicle basis (Franco et al., 2013; Khan and Frey, 2018). However, the PEMS method cannot measure secondary pollutants due to sampling directly from the tailpipe, and its high cost limits its broad application across entire vehicle fleets.

Alternative real-world measurements that do not require physical interaction with the vehicle include remote sensing (including roadside measurement), vehicle chasing, and tunnel studies. In all of these measurements, emissions are sampled after their release into the atmosphere either at the side or above to road (remote sensing/roadside measurement), downwind on the road (chasing) or at the entrance and exit of traffic tunnels. Chase studies involve a mobile air quality laboratory following target vehicles while driving to measure their emissions. This has the advantage of capturing a wide range of vehicle operating conditions without physically interfering with the vehicle, but the cost is typically very high and the number of vehicles that can be sampled is very limited (Franco et al., 2013). Tunnel measurements involve pairing traffic counting with air pollution sampling at tunnel entrance and exits to develop fleet-based emissions estimates.

Remote sensing/roadside measurement involves installing instruments for measuring vehicle emissions at the roadside to capture emissions and optionally vehicle data via cameras. Measurement typically only occurs at one location, potentially missing emissions across the full range of driving conditions and can be subject to more influence from the environmental conditions such as wind direction (Breuer and Burgard, 2019; Burgard et al., 2011; Franco et al., 2013; Hilker et al., 2019; Ropkins et al., 2017; Wang et al., 2018a). This method has mostly been applied by regulatory agencies, typically at a small number of locations due to the complex operation and high cost of the instruments (Johnson and Joshi, 2017; Ke et al., 2013; Lu et al., 2011; Moltchanov et al., 2015). Despite these limitations, a growing number of research studies have been done using roadside measurement. Zimmerman et al. (2016) applied road-side measurement to measure individual vehicle emissions from gasoline direct injection (GDI) engines. Wang et al. (2015) used high-time resolution (< 10 sec) roadside measurement and

subsequently identified emissions plumes from the vehicle fleets to calculate emission factors. Hiker et al. (2019) applied roadside measurement at a slower time resolution (hourly) the difference between sites. As such, there is evidence that roadside measurement may be a useful tool for assessing vehicles at different scales, from the individual vehicle to fleet-wide. The different emissions monitoring approaches are summarized in Table 2.2.

Table 2.2 Comparison of different emissions monitoring approaches.

Type	Advantages	Drawbacks
Laboratory: Dynamometer (engine or chassis)	<ul style="list-style-type: none"> • Precise • Range of operating conditions • Repeatability 	<ul style="list-style-type: none"> • Very expensive (\$\$\$), • Time intensive, • Limited number of vehicles tested
Real-world: Chasing	<ul style="list-style-type: none"> • Measure secondary PM • Large # of vehicles 	<ul style="list-style-type: none"> • Very expensive (\$\$\$) • Safety considerations
Real-world: Tunnel studies	<ul style="list-style-type: none"> • Large # of vehicles • Track trends over time 	<ul style="list-style-type: none"> • Fleet-specific (not vehicle specific) • Limited range of vehicle operation
Real-world: On-board PEMS	<ul style="list-style-type: none"> • Range of operating conditions • Simple to use • Relatively inexpensive 	<ul style="list-style-type: none"> • Limited # of vehicles that can be tested • Added mass (30-70 kg)
Real-world: Remote sensing	<ul style="list-style-type: none"> • Large # of vehicles (1000s/day) • ID high emitters quickly 	<ul style="list-style-type: none"> • Snapshot at a location • Limited variability in vehicle operation • High uncertainty

Some studies have compared the different real-world emissions monitoring approaches. In Ropkins et al. (2017), a new laser-based remote sensing roadside instrument was compared with PEMS. The result indicates a good correlation between the actual gas concentration and measurement results with r^2 of 0.97 and slope of 0.71. In an urban campaign conducted by Huang et al. (2018), the potential capability of remote sensing systems to identify high emitters was demonstrated but the author acknowledged the uncertainty in whether this method could be as convincing as PEMS whose accuracy is closer to in-lab testing.

Increasingly, regulatory agencies are incorporating real-world emissions testing requirements into their policies and programs. Given the identified mismatch between laboratory and real-world testing, and the possibility to cheat regulations as seen with the Volkswagen scandal, real-world monitoring has fewer blind spots when it comes to law enforcement. Europe is now working on applying the PEMS test to light-duty vehicles (LDVs) to enforce future emission legislations, and heavy-duty vehicles (HDVs) have already been required to go through PEMS testing procedures since 2009 (Vlachos et al., 2019). The United States Environmental Protection Agency (U.S. EPA) is also conducting small-scale PEMS tests with in-use vehicles (Nam and Mitcham, 2019). Though not as repeatable standardized as laboratory tests, real-world emission tests are still promising testing programs in the future.

One area of promise in this regard is the use of low-cost air quality sensors (discussed more fully in Section 2.6). Recently, researchers have started to use low-cost sensors near roadsides and across urban areas. This new technology could allow us to have sensors with a much lower price at a reasonable accuracy (Zimmerman et al., 2018). It is possible that with the help of low-cost sensors, high-density roadside monitoring networks could be constructed to capitalize on the advantages of roadside measurement while reducing the total cost (Hasan et al., 2018; Johnson and Joshi, 2017; Ke et al., 2013; Lu et al., 2011). The data from high-density roadside monitoring networks could offer promising solutions for several challenges from identifying high emitters to assessing the outcomes of related environmental policies.

2.5 Emissions Reduction Strategies

2.5.1 After-treatment

New combustion technologies and after-treatment technologies have long been used to reduce pollutants from on-road vehicles (Thurnheer et al., 2011; Jang et al., 2015; Bonatesta et al., 2014; Zhu et al., 2016; Johnson and Joshi, 2017a). The effectiveness of after-treatment technologies is well proven by laboratory experiments using both engine and vehicle dynamometers. Emission control technologies can be divided into 2 streams, particulate pollutant control and gaseous pollutant control. Diesel vehicles and GDI-powered vehicles are the primary sources of PM emissions. To suppress PM emissions, for both diesel and GDI vehicles, the most common way is to install particulate filters, such as a diesel particulate filter (DPF) in the after-treatment system. DPF filtration efficiencies typically range from 70% to 100% (Johnson and Joshi, 2017; Wang et al., 2014). For gaseous pollutants, diesel vehicles and gasoline vehicles have different strategies due to differences in their air-to-fuel ratio. Gasoline engines typically work at the stoichiometric air-fuel ratio, and as such, the three-way catalyst (TWC) is the most widely applied system to reduce CO, hydrocarbons (HC), and NO_x. For diesel engines working at lean air to fuel ratios, catalytic reduction (SCR) is typically used to reduce NO_x and oxidation catalysts are used to oxidize CO and HCs. An important characteristic of the TWC in gasoline vehicles is that the conversion efficiency of the TWC is lower when the temperature is below the light-off temperature, so one of the directions of current studies on vehicle emissions is cold start emissions when the TWC is at a lower temperature (Bielaczyc et al., 2014; Cédric et al., 2016; Khan and Frey, 2018; Yao et al., 2012).

2.5.2 Other approaches

There are a variety of other approaches aside from after treatment to reduce emissions. Some studies have shown that emissions could be reduced by optimizing the driving behaviours (Çolak et al., 2016; Fan and Perry, 2018; Rakha et al., 2000). In Rakha et al. (2000), speed and acceleration were identified as factors influencing vehicle emissions. The results prove that acceleration has a significant influence on the emissions, indicating the possibility of reducing emissions by optimizing the acceleration. In the work of Lin et al. (2015), the influence of the traffic delay at intersections on vehicle emissions have been quantified. They find that by reducing traffic delay, or in other words, making the vehicles pass smoothly at intersections, the emissions are reduced. Apart from the modification of driving behaviours and after-treatment systems, researchers are also trying to make changes to the operating modes of the vehicle to reduce emissions. Hybrid vehicle technologies could reduce emissions by optimizing engine working conditions (Zhang et al., 2020; Thomas et al., 2020). Also, traffic control strategies could have a significant influence on emission reductions, by reducing idling time and average acceleration (Lin et al., 2015).

2.6 Low-cost air pollution sensors

2.6.1 Characteristics of low-cost sensors

Traditionally, measurement of air pollutants relies on high-cost reference-grade instruments, whose costs start from \$1000-\$20,000 USD to measure one criteria air pollutant (Clemitshaw, 2010; Zimmerman et al., 2018; Snyder et al., 2013). Reference-grade instruments have the advantage of being accurate, however, they are typically complex instruments, requiring professional operation (Mead et al., 2013). Regulatory instruments are far more difficult to deploy within a larger air pollution monitoring network, such as what might be needed to measure the

emissions of the real-world transportation system (Chong et al., 2003), due to weatherproofing, power demands and large size limitations. As such, existing regulatory monitoring networks have typically relied on a few, spatially widespread sensing locations. To quantify the air quality impacts of vehicles, a high spatial-density monitoring network, as well as real-time data, are needed since vehicle emissions vary dynamically in both space and time, depending on weather, road conditions, maintenance, fuel, and how the vehicle is operated (Kumar et al., 2015).

With new lower-cost sensing technology comes the opportunity to build a high spatial-density monitoring network capable of measuring multiple pollutants at a significantly lower cost (Zimmerman et al., 2018; Masson et al., 2015; Doherty et al., 2006). Commercially available low-cost air pollution sensors are dominated by a few technologies including light-scattering particle matter sensors and electrochemical or metal oxide gas sensors (Maag et al., 2018). Over the past few years, intensive research has been done to characterize and develop low-cost particle and gas sensors. In Budde et al. (2018), a low-cost particle sensor was tested and was found to have a strong reliance on relative humidity and poorer detection of smaller particles. In Kelly et al. (2017), an assessment of a low-cost particle sensor showed that the sensor was more influenced by properties of the particulate matter (e.g, composition) than typical research instruments while also having good accuracy during an in-lab test. Studies on low-cost gas sensors have mostly demonstrated that the gas sensors are influenced by the environmental conditions as well as other pollutant cross-sensitivities (Maag et al., 2018; Zimmerman et al., 2018; Pang et al., 2018; Malings et al., 2019). In Hossain et al, the cross-sensitivity between NO_x and O_3 was addressed with a pair of sensors (Hossain et al., 2016), however, it remains uncertain whether other gases may interfere

with the measurement. The long-term stability and selectivity could also change as electrolytes degrade or metal oxide sensors undergo irreversible reactions (Yang et al., 2019).

Recently, some mature low-cost air pollution sensors have been made commercially available which combine a group of sensors with data acquisition systems and remote data transmission modules. Using these remote data transmission modules, data can be easily uploaded on customer servers, providing users with convenience to collect and analyze large data sets with little to no in-person interaction. Still, low-cost sensors have ongoing accuracy challenges compared to reference-grade instruments (US EPA Tier 5 data quality). However, with the new calibration methods, the accuracy of low-cost sensor could meet the requirements of certain purposes outlined by US EPA, such as hotspot identification (Tier 2) and supplementary monitoring (Tier 4) (Mead et al., 2013; Cross et al., 2017; Malings et al., 2019; Zimmerman et al., 2018). The user-friendly and budget-friendly nature of low-cost sensors, combined with new calibration approaches (Section 2.6.2), could support the collect the real-time emissions profile of vehicles across cities. With a larger sensor network, the real-time data could provide important information on the air quality impacts of traffic management technologies and help characterize vehicle fleets (Kumar et al., 2015).

2.6.2 Calibration techniques

Due to the cross-sensitivity and sensitivity to environmental factors of the low-cost sensors mentioned in Section 2.6.1, calibration must be conducted before or during the measurement with low-cost sensors (Zimmerman et al., 2018). Electrochemical gas sensors have been shown to have cross-sensitivity between NO_x and ozone, as well as between CO and molecular hydrogen as a

first-order effect (due to redox reactions) and ambient temperature (affects diffusion coefficient) and relative humidity (affects condensation on potentiostat electronics) as a second-order effect (Mead et al., 2013; Zimmerman et al., 2018). A first-order effect is essentially chemical interference that directly affects the current in the sensor circuit, which can be hard to resolve with linear models. More complex models, including random forests and artificial neural networks, have been introduced to address this effect. A second-order effect does not directly change the current, but it affects the chemical reaction rate and subsequent current generation which then influences concentrations. The second-order effect has been well addressed with linear models (Maag et al., 2018; Malings et al., 2019; Zimmerman et al., 2018). Malings et al. (2020) demonstrated that low-cost PM sensors also require calibration due to the influence of relative humidity, particle hygroscopicity, and temperature. Earlier research indicated an even wider range of cross-sensitivities between electrochemical sensors and that exposure to cross-sensitive species had long-lasting ‘memory’ effects (Austin and Goyer, 2006). Even when the sensors receive factory calibration by the manufacturer, it has been shown that these calibrations are not robust over time and regular calibration should be done to ensure the accuracy (Hodgson et al., 1999; Cavellin et al., 2016; Papapostolou et al., 2017). To address this, there has been ongoing research on calibration approaches and how frequently calibration algorithms should be updated.

Different methods have been developed for low-cost sensor calibration. Linear regression models are the most straightforward method. These models assume linearity between the increments of low-cost sensor signal response and the change in actual concentrations (Maag et al., 2018). However, linear regression models are poorly suited to sensors that are influenced by a variety of factors in the ambient environment (Castell et al., 2017). During the calibration of electrochemical

gas sensors, according to Zimmerman et al. (2018), the linear regression model only worked well on CO sensors (Pearson R of 0.91). Castell et al. (2017) further indicate this method could not make the low-cost sensors suitable for monitoring due to the low accuracy post-calibration. Some research has shown a reasonable performance of low-cost sensors with linear regression calibration models in the laboratory. However, the work of Esposito et al. (2016) indicates that the calibration accuracy decreases significantly when moving from the lab to the field. The linear regression model is more likely to be accepted as a factory calibration method rather than being applicable to air pollution monitoring or even research purposes. As an extension of the simple linear regression model, multiple linear regression models including other pollutants and meteorological parameters such as temperature and relative humidity have been explored (Maag et al., 2018; Malings et al., 2019; Zimmerman et al., 2018). Despite including more parameters, the consensus is that multiple linear regression calibration models do not provide satisfactory performance except for PM sensors which use light scattering (Malings et al., 2020).

It has been hypothesized that the poor performance of multiple linear regression models is due to nonlinearity in sensor response to cross-sensitive pollutants or environmental conditions. Being more capable of handling nonlinearity, machine learning calibration methods have been another popular method accepted in real-world research. The machine learning models mostly use the signal from a sensor array (including temperature and relative humidity) as the predictors and use these models to reproduce complex relationships between different input factors (Maag et al., 2018; Malings et al., 2019). Lewis et al. (2016) applied boosted regression trees and Gaussian process emulation to sensor calibration and found that the corrected signal replicated the concentrations measured by reference-grade instruments well. De Vito et al. (2009) applied

artificial neural network models to a low-cost sensor system for measuring NO_x, CO and CO₂. They found that an artificial neural network model could maintain accuracy stability within an acceptable range. Recently, Zimmerman et al. (2018) introduced random forest models into sensor calibration of NO_x, CO, CO₂, and O₃ sensors and tested these algorithms in long-term studies spanning 16 months. Malings et al. (2019) then went on to develop a comprehensive evaluation framework and also concluded that the random forest model had similar performance to artificial neural network model calibrations when calibrating the same dataset, however the random forest model was slightly more consistent across different sensing units.

2.7 Conclusions

Vehicle emissions are a complex mixture ubiquitous in urban environments with significant negative impacts on air quality and human health. Countries around the world have been making more stringent emission regulations and encouraging the development and application of emission reduction technologies. From optimizing the combustion process in the engine to optimizing traffic management, different methods have been taken to reduce vehicle emissions.

These reductions have generally been mandated by increasingly strict vehicle emissions policies that require a range of tests, and increasingly, assessment of emissions in a real-world context. However, widespread real-world measurement approaches are limited by the instrument limitations (size, power), costs and the complexity of operation. Low-cost air pollution sensing technologies may be a promising alternative for the measurement of real-world vehicle emissions. These tools could increase the coverage of emission measurement and air quality monitoring. Ideally, the low-cost sensors could provide researchers with high spatial and temporary density

measuring results to convert the pollutant signal into meaningful metrics such as vehicle emissions factors. Though low-cost sensors noted accuracy limitations, new calibration methods have been developed to enable more accurate readings. As such, with low-cost sensors, a vehicle emission measurement network could be developed, and the real-world emissions of the vehicle fleet could be fully characterized. The data from such a network could be used to assess the impact of vehicle emission regulations, for instance, nation-wide fleet emission factors could be developed, and could then be used to evaluate the impact of the policy. Also, this method could potentially be applied to identify high-emitting fleets. Subsequent policies targeting that specific fleet could be put forward to reduce emissions more efficiently. Apart from policy assessment, we could apply this method to evaluate the change of vehicle emissions with new technologies, for instance, connected vehicles. However, this is all contingent on low-cost sensors having adequate measurement sensitivity to detect vehicle emissions. The subsequent chapters will explore this idea in a controlled parkade setting (Chapter 4) following instrument calibration (Chapter 3).

Chapter 3: Instrumentation and Calibration

3.1 Introduction

In this chapter, the primary instrument used in this study is introduced, the Real-time Affordable Multi-Pollutant (RAMP, SENSIT Technologies), a monitor composed of multiple commercially available low-cost sensors. One of the essential steps of this work is to improve the accuracy of low-cost sensing instruments for vehicle emission measurement. The calibration models needed for this assessment have been developed (trained) and evaluated in this chapter. The calibration of the RAMPs was based on a three-week collocation with regulatory-grade instruments at a near-road monitoring station (Section 3.3.1). In this work, a machine-learning random forest (RF)-multiple linear regression (MLR) hybrid model was developed and applied to correct the data collected by the RAMP gas sensors following the approach of Malings et al. (2019) and Zimmerman et al. (2018), which evaluated these models extensively (Section 3.3.2).

Temperature and relative humidity are two known factors that cause disagreement between reference-grade PM sensors and low-cost optical PM sensors since most optical low-cost PM sensors report data at ambient conditions while reference-grade PM monitors have rigid requirements for temperature (20-23°C) and relative humidity (30%-40%) (Malings et al., 2020; USEPA, 2016). Accordingly, PM_{2.5} mass concentration was corrected with a multiple linear regression model (Malings et al., 2020) with the predictors being sensor-reported PM_{2.5} mass concentration, relative humidity, and temperature in this work (Section 3.3.3). The performance of the calibration models was assessed on three days of independent testing data not used in the calibration model building.

3.2 Real-time Affordable Multi-Pollutant Monitor

In this study, we used the Real-time Affordable Multi-Pollutant (RAMP, SENSIT Technologies) monitor (Figure 3.1, Figure 3.2). The RAMP contains commercially available low-cost sensors for measuring PM_{2.5}, NO, NO₂, CO, O₃ and CO₂ (Table 3.1) within a weather-proof shell (Zimmerman et al., 2018). The sensors are passive (no active airflow) with no conditioning processes. Details of the RAMP have been described in detail elsewhere (Malings et al., 2019; Zimmerman et al., 2018) but are described here briefly.

Table 3.1 Configurations of the sensors inside the RAMP monitor.

Measurement (Unit)	Sensing method	Serial number (Manufacturer)
CO (ppb)	Electrochemical (with auxiliary and working electrodes)	CO-B41 (Alphasense)
NO (ppb)		NO-B4 (Alphasense)
NO ₂ (ppb)		NO2-B43F (Alphasense)
O ₃ (ppb)		Ox-B431 (Alphasense)
PM _{2.5} (µg/m ³)	Laser scattering	PA-II (Plantower)
CO ₂ (ppm)	Nondispersive infrared (NDIR)	SST CO ₂ S-A (SST Technologies)
Temperature (°C)*	Bandgap	
Rel. Humidity (%)*	Capacitive	

* Temperature and relative humidity measurements are built-into the CO₂ sensor

The electrochemical gas sensors used in this study work by acquiring the current generated by the reduction-oxidation reaction between the target gas and the electrode. The NDIR sensor used in this study measures the absorption ratio of infrared light to determine the concentration of CO₂. The PM sensor uses a light-scattering technique, based on the principle that the direction of light will be changed when it meets small particles and the light diffracted (scattered) by the proportional to the concentration of particles. The reacting time of the sensors varies from 15 to 90 seconds.



Figure 3.1 RAMP mounted in a parking garage (right) and the bottom of a RAMP monitor showing the location of the sampling units (left).

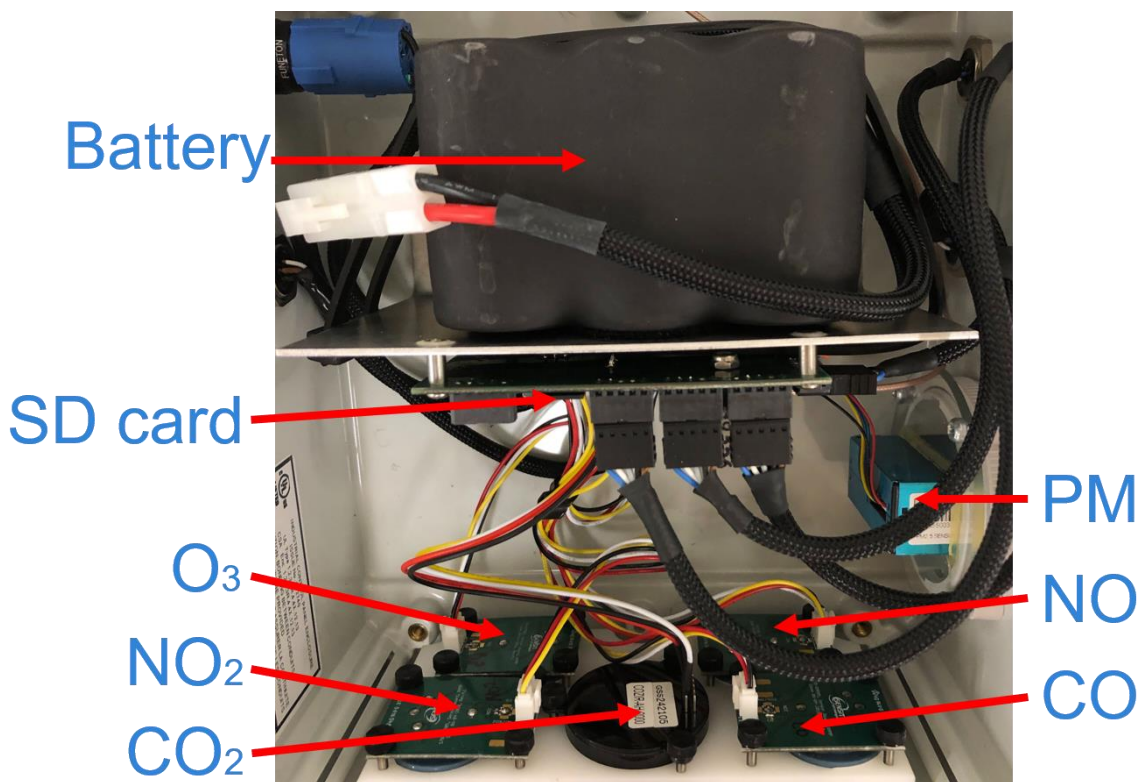


Figure 3.2 Picture inside the weather-proof shell of the RAMP, each low-cost sensor is marked with the target it measures. The sensors inside this package are independent of each other and could be replaced quickly when damaged.

The RAMP can use external power or a built-in rechargeable battery which supports approximately 5 days of measurement with all sensors operational. A built-in customized data acquisition and

control system measures the analog signal from the sensors, conditions the analog output with filtering circuitries removing noise signatures and converts the conditioned analog signal to a digital signal which becomes the final output. These outputs are uploaded wirelessly (using cellular networks) to an online server enabling remote monitoring. The data is also saved on an SD card inside the monitor for backup (Zimmerman et al., 2018). The RAMP records data with a 15-second sampling resolution. This was down-sampled to 5 min averages to increase the signal-to-noise ratio (Li et al., 2019; Zimmerman et al., 2018).

Typically, the output of the gas sensors is influenced by various factors including relative humidity (RH), temperature (T), and cross-sensitivities to other pollutants that increase the uncertainty (Mead et al., 2013). For example, the NO₂ sensor output is influenced by RH (affects condensation on potentiostat electronics), T (affects diffusion coefficient) and also the concentrations of O₃ and other gases (due to conflicting redox reactions) (Zimmerman et al., 2018). The accuracy of low-cost optical PM sensors signal is affected by the omission of particles smaller than minimum detectable size (<300 nm) as well as the influence of T and RH, all of which can cause a discrepancy between the measurement result and measurements with reference grade instruments (Malings et al., 2020). As such, calibration is needed for both the gas phase and PM sensors. The calibration methods are discussed in Section 3.3.

3.3 Sensor Calibration

3.3.1 Collocation Campaign

Calibration was based on a three-week collocation with regulatory-grade instruments at the Clark Drive Near-Road Monitoring Station operated by Metro Vancouver, the air quality regulatory

authority in the region. The Clark Drive site, shown in Figure 3.3, is within 15 m of a major intersection and is disproportionately impacted by traffic-related air pollution, making it an ideal calibration location. The reference-grade instruments equipped at Clark Drive site are listed in Table 3.2.

Table 3.2 Configurations of the sensors at Clark Drive site.

Measurement (Unit)	Sensing method	Manufacturer (Serial number)
CO (ppb)	Filter correlation infrared	Thermo Scientific (48i-TLE)
CO ₂ (ppm)	Nondispersive infrared	LI-COR (840A)
NO (ppb)	Chemiluminescence	Thermo Scientific (42i)
NO ₂ (ppb)		
O ₃ (ppb)	UV photometric	Thermo Scientific (49i)
PM _{2.5} (µg/m ³)	Nephelometer	Thermo Scientific (SHARP5030)

The filter correlation infrared CO sensor compares the difference between the absorption rate of the sample and the pure target gas to determine the concentration of the target gas in the sample.

The chemiluminescence NO_x sensor uses the emission of light during the reaction between NO and O₃. The light will be measured to determine the concentration of NO. After the determination of NO, the same process will be repeated with NO₂ converted into NO and the difference between the new measurement and previous NO concentration is used to calculate the NO₂ concentration.

The UV photometric O₃ sensor determines the concentration of O₃ by comparing the difference of absorption rate between sample gas and sample gas without O₃. The nephelometer measure the light reflected by the particles in the sample air to determine the concentration of PM_{2.5}.

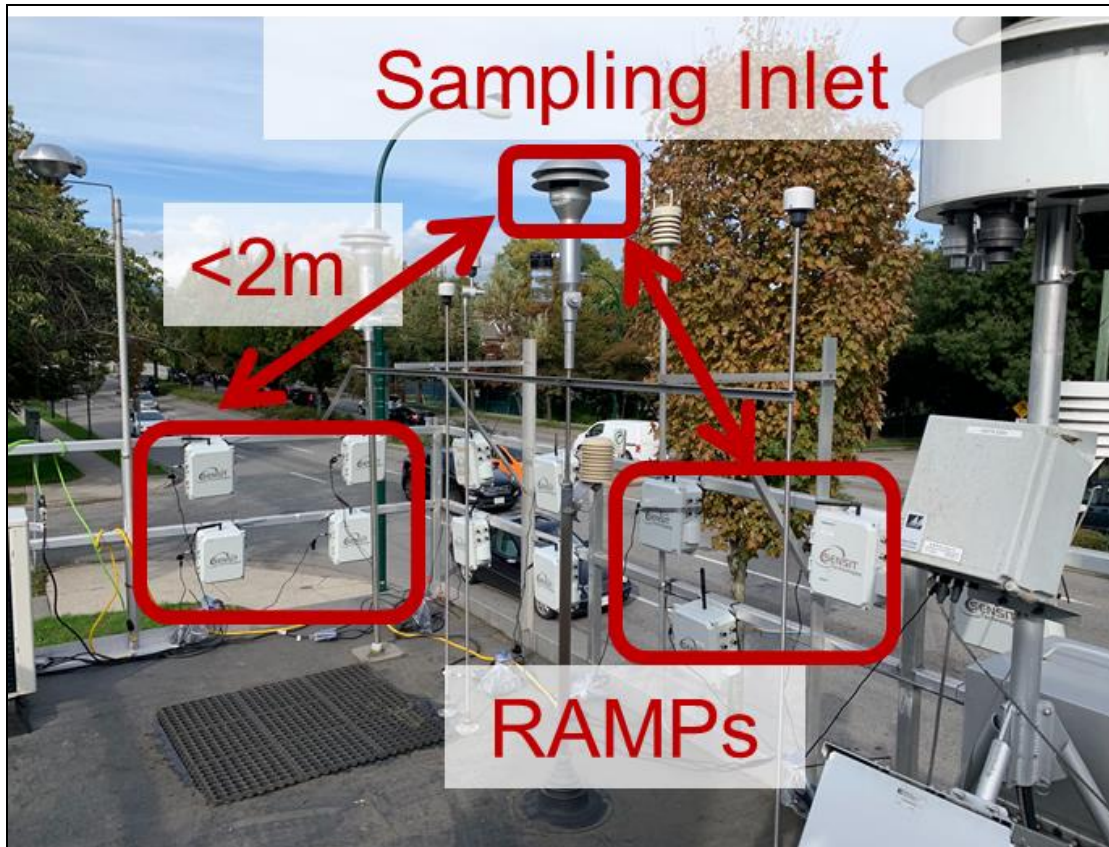


Figure 3.3 Picture of the collocation site at Clark Drive in Vancouver, BC beside a major roadway the sensors are deployed close to (within 2 meters) the sampling pipe of reference-grade instruments. The primary monitoring target of this site is the emissions from vehicles passing by.

The collocation campaign started on September 24th and ended on October 11th in 2019. The collocation data from September 24th to October 8th was selected as a training dataset and the rest of the collocation data was used for evaluation of calibration results.

The calibration results normally retain their quality and consistency for around 4 months (Malings et al., 2019; Zimmerman et al., 2018), while there have been no further studies testing the further accuracy change in longer-term. As such, for this study, the calibration model is expected to remain

valid. However, in general, it's recommended that the calibration process be repeated as frequently as is reasonably possible.

3.3.2 Calibration of Gas Sensors

3.3.2.1 Random forest (RF) model

The random forest model was first introduced to the calibration of low-cost sensors by Zimmerman et al. (2018) and is described briefly here. The RF model is essentially an ensemble of decision trees and each decision tree is composed of many nodes. In this study, the forest is composed of 100 decision trees. In a decision tree, each parent node splits into its child nodes by considering a random subset of predictive variables (m_{try}) until reaching the terminal nodes. In this study, the number of predictive variables in the random subset (m_{try}) considered in generating the child nodes are tuned by the user to reach the minimum root mean square error (RMSE) and one predictive variable is selected from the subset based on how well it could predict response. Here, the m_{try} was set to include all possible variables ($n=7$). This process is repeated for each split between a parent node and a child node until a terminal node is reached. Here, the terminal node was reached when the node contained 5 data points. Each decision tree is formed in the training process with random datapoints bootstrapped from the training dataset. When predicting the results, the input data will be applied to every decision tree and the results from all of the decision trees will be averaged to give the final predicted result.

3.3.2.2 Hybrid model

The calibration model of gases is based on a hybrid random forest (RF)-multiple linear regression (MLR) model developed by Malings et al. (2019). The purpose of a hybrid RF-MLR calibration

model is to account for the RF model's inability to extrapolate outside of the training concentration range. To develop a hybrid model, RF and MLR calibration models are constructed separately and then an algorithm is written to switch from the RF model to the MLR model if the model outputs are close to the boundary of the training range. Both the RF and MLR models used the same predictors (CO₂, CO, NO, NO₂, O₃, relative humidity, and temperature) and the cut-off point to switch from RF to MLR was optimized using an exploratory analysis to maximize overall calibration accuracy. Calibration model performance was assessed on three days of independent testing data not used in the calibration model building.

The random forest model is expressed in Equation (3.1) where CO is used as an example, RH stands for relative humidity and T stands for temperature.

$$CO_{Corrected} = F_{RF}(CO_{2\ Original}, CO_{Original}, NO_{Original}, NO_{2\ Original}, O_{3\ Original}, RH, T) \quad \text{Eq. (3.1)}$$

The MLR model is expressed in Equation (3.2) where CO is used as an example:

$$CO_{Corrected} = \beta_0 + (\beta_1 * CO_{Original}) + (\beta_2 * T) + (\beta_3 * RH) \quad \text{Eq. (3.2)}$$

Overall, a unique model was been trained for each sensor in every sensor package. Each RF model was trained with 100% of the training dataset. The part of the training data corresponding to the top 10th percentile of the output of RF model was used to train the MLR model since the goal of the MLR model was to accurately predict at higher concentrations. When applying the hybrid

model, all data is first corrected by RF model, it will then switch between the RF model and the MLR model by determining whether the output of RF model exceeds the cut-off value.

To find out this cut-off value, we first determine the percentile of the RF model's output results where the RF models lose accuracy and that percentile is referred to as the 'upper percentile', and the corresponding output value of RF model at upper percentile is referred to as the 'cut-off value'. The optimal percentile was determined by evaluating overall model performance with cut-point percentiles ranging from 90 to 99%. In this study, 98% has been determined to be the optimal percentile where the RF models lose accuracy. The parameters used to make this evaluation were the coefficient of variation of the mean absolute error (CvMAE, essentially mean absolute error normalized by the average concentration) and the Pearson correlation coefficient (Pearson R) during the evaluation of the calibration on the testing data. CvMAE and Pearson R are calculated according to Equations (3.3) and (3.4). As is shown in Figure 3.4 for the CO models, the R^2 approaches a maximum when the model switches from RF to MLR at the 98th percentile of the training data.

$$\text{Pearson R} = \frac{\varepsilon[(\text{Predicted} - \mu_{\text{Predicted}})(\text{Reference} - \mu_{\text{Reference}})]}{\sigma_{\text{Predicted}}\sigma_{\text{Reference}}} \quad \text{Eq. (3.3)}$$

Pearson R mainly assesses the linear correlation between corrected data and the corresponding reference data. In the equation, ε stands for the expectation, $\mu_{\text{predicted}}$ stands for the mean of predicted dataset and $\mu_{\text{Reference}}$ stands for the mean of the reference dataset. CvMAE is calculated as:

$$CvMAE = \frac{1}{\text{Avg. Reference}} \times \left[\frac{1}{n} \sum_{i=1}^n |\text{Predicted}_i - \text{Reference}_i| \right] \quad \text{Eq. (3.4)}$$

Avg. Reference stands for the average value of the reference data, Predicted_i , and Reference_i stand for the i th datapoint in the predicted dataset and reference dataset respectively. The results of the calibration are shown in Figure 3.5.

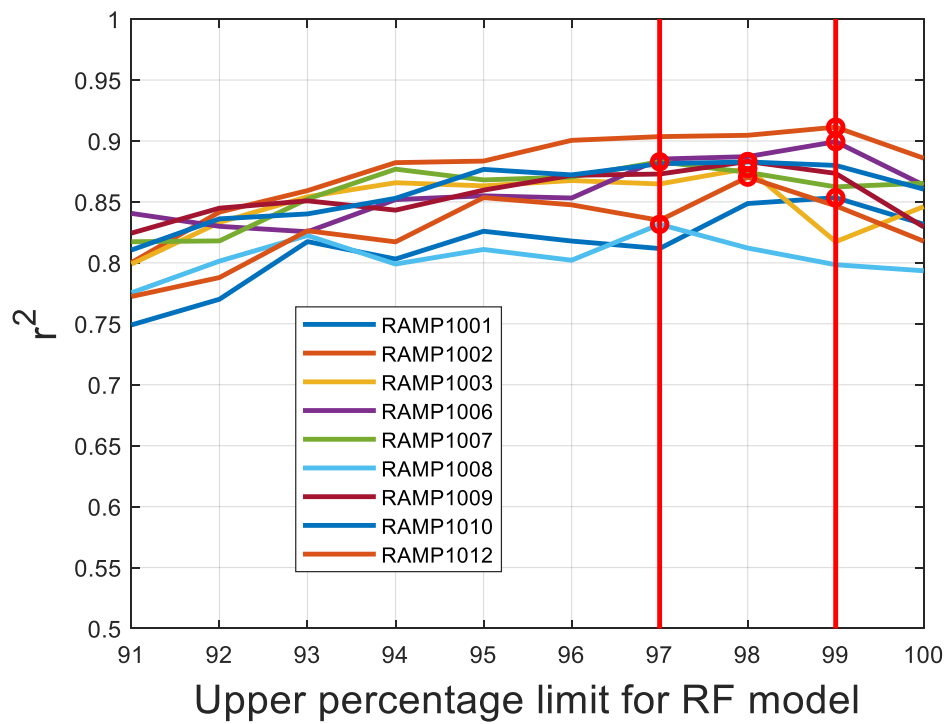


Figure 3.4 Determination of the cut-off point for switching from the random forest model to the MLR model based on changes to r^2 . In this case, the r^2 is approaching the greatest value when the upper percentage limit for the RF model is around 98%, thus 98% is selected.

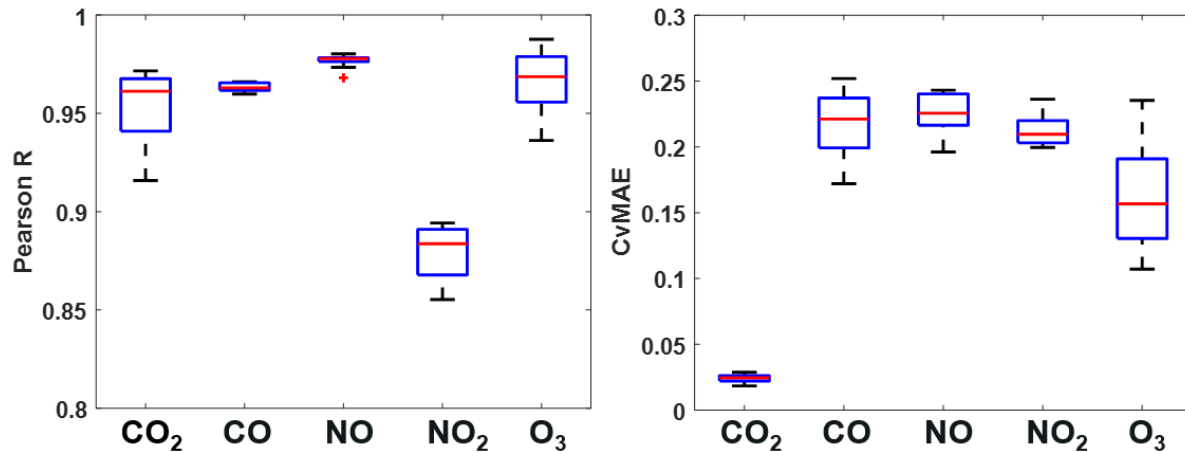


Figure 3.5 Performance of the calibration models on the withheld testing data for the gas sensors of all of the RAMPs in this study. CvMAE is the coefficient of variation of the mean absolute error (i.e., the mean absolute error normalized by the average concentration). CvMAE can be interpreted as the approximate percent error (e.g., ~ 15% for ozone). For the box plots, whiskers are 10th and 90th percentile, box edges are 25th and 75th percentiles, and the line is the median.

Based on the previous similar work of RAMP calibration with a random forest model by Zimmerman et al. (2018) and Malings et al. (2019), our calibration achieved similar or better performance. The comparison between the previous study and this work is provided in Table 3.2. Though NO sensor was not assessed in the past studies, the NO sensor showed similar CvMAE and Pearson R values as other pollutants, suggesting the calibration similarly successful as the other pollutants. Putting the results in the context of EPA air quality sensor performance guidelines, the error is still too high for regulatory monitoring, which requires the error to be less than 7% to 15% (USEPA, 2016). However, the current target of this initial study is to explore the method to measure vehicle emissions. Further studies are expected to characterize the uncertainty in full detail.

Table 3.3 Comparison of Calibration Results between our attempt and the original results published by Zimmerman et al. (2018) and Malings et al. (2019).

		Average Pearson R	Average CvMAE
CO	This study	0.96	21.7%
	Zimmerman et al. (2018)	0.95	14%
	Malings et al. (2019)	0.88	20%
NO₂	This study	0.88	21.2%
	Zimmerman et al. (2018)	0.82	29%
	Malings et al. (2019)	0.69	42%
CO₂	This study	0.95	2.4%
	Zimmerman et al. (2018)	0.88	2.2%
O₃	This study	0.97	18.8%
	Zimmerman et al. (2018)	0.93	15%
	Malings et al. (2019)	0.9	22%

3.3.3 Calibration of PM_{2.5} Sensor

Temperature and relative humidity are the first two factors that cause the disagreement between reference grade PM sensors and low-cost optical PM sensors since most optical low-cost PM sensors report data at ambient conditions while the reference-grade PM has rigid requirement on temperature (20-23°) and relative humidity (30%-40%) (Malings et al., 2020; U.S. Environmental Protection Agency, 2016). Accordingly, PM_{2.5} mass concentration was corrected with a multiple linear regression model (Malings et al., 2020) with the predictors being PM_{2.5} mass concentration, relative humidity, and temperature in this study. The calibration results are evaluated with the same criteria as Section 3.3.2 and are shown in Figure 3.6.

$$CO_{Corrected} = \beta_0 + (\beta_1 * PM_{2.5_{Original}}) + (\beta_2 * T) + (\beta_3 * RH) + (\beta_4 * DP(RH, T)) \quad \text{Eq. (3.5)}$$

Though Malings et al (2020) provided a set of β coefficients based on reference monitor collocation in Pittsburgh, we independently fit our own β coefficients based on a Vancouver collocation. Our model coefficients were of a similar magnitude and direction to those calculated in Malings et al. (2020). In Equation (3.5), DP stands for dew point at a certain relative humidity and temperature. The DP is calculated with one form of the Magnus-Tetens Formula (Camuffo et al., 2018; Dario, 2019) due to its appropriateness at room temperature conditions, similar to our study, as per equations (3.6) and (3.7).

$$\gamma(T, RH) = \ln\left(\frac{RH}{100}\right) + \frac{bT}{c + T} \quad \text{Eq. (3.6)}$$

$$DP = \frac{c\gamma(T, RH)}{b - \gamma(T, RH)} \quad \text{Eq. (3.7)}$$

Where T and DP are in Celsius, RH is in percentage, $b=17.62$, $c=243.12^\circ\text{C}$ (Camuffo et al., 2018; Dario, 2019). The results of the $\text{PM}_{2.5}$ calibration are shown in Figure 3.6.

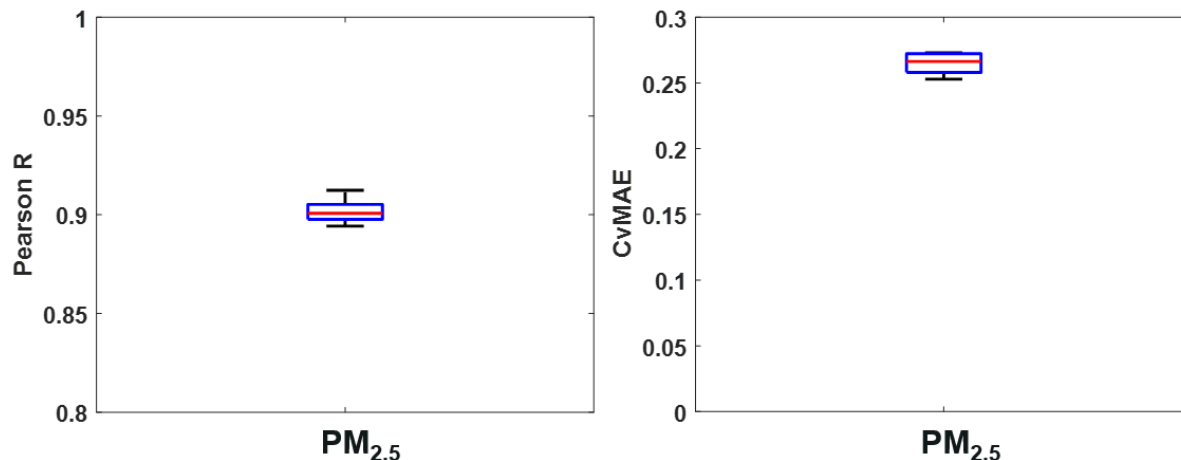


Figure 3.6 Performance of the calibration models on the withheld testing data for the $PM_{2.5}$ sensors of all of the RAMPs in this study. CvMAE is the coefficient of variation of the mean absolute error (i.e., the mean absolute error normalized by the average concentration). CvMAE can be interpreted as an approximate percent error. For the box plots, whiskers are 10th and 90th percentile, box edges are 25th and 75th percentiles, and the line is the median.

The results of $PM_{2.5}$ sensor calibration was compared with the previous work by Malings et al. (2020) in Table. Generally, the Pearson R and CvMAE were close to the previous results. But the results still cannot meet the standard of regulatory monitoring (<10% error for $PM_{2.5}$).

Table 3.4 Comparison of $PM_{2.5}$ Calibration Result between our attempt and the original results published by Malings et al. (2020).

	Average Pearson R	Average CvMAE
This study	0.9	27%
Malings et al. (2020)	0.91	14%

3.4 Conclusions

In this chapter, we briefly described the primary instrument used in this study, the RAMP. Its small size and ability to measure multiple pollutants suggest it may be applied to vehicle emission measurement. To calibrate the sensors, the calibration procedures designed by Zimmerman et al. (2018), Malings et al. (2019) and Malings et al. (2020) were adopted. We found the results of the calibration mostly match the previous studies.

Chapter 4: Development of Vehicle Fleet Emission Factors in Parkades

4.1 Introduction

As introduced in Chapter 2, one potential application of widespread low-cost sensor deployment is using LCS systems as a remote sensing tool for the measurement of fleet-based emission factors (EFs). If these tools could be used for this purpose, low-cost sensor systems could be deployed at hundreds of locations to capture a broad range of vehicle operating conditions and environments, generating millions of vehicle plumes for analysis. However, it remains uncertain if the measurement sensitivity of low-cost sensor systems is capable of such measurements.

To address this question, this chapter assesses the suitability of the RAMP low-cost sensor systems for determining fleet-based EFs using a remote-sensing-type approach. In this study, we deployed 6 low-cost monitors in 3 parking garages on the University of British Columbia (UBC) campus in Vancouver, British Columbia for three months. These traffic-rich environments combined with vehicle counting data provided by UBC Parking Services enabled us to develop our method with some built-in validation. The calculated EFs are then compared to the published literature.

4.2 Measurement Sites

4.2.1 Physical Features of Sampling Locations

Three parking garages operated by UBC Parking Services were sampled in this study. A short description of the sites is provided in Table 4.1. For simplicity, the three parking garages will be henceforth referred to as AG1 and AG2 (above-ground parking garages 1 and 2) and BG1 (below-ground parking garage 1).

Table 4.1 Characteristics of the parking garages.

Garage Name	Location	Ventilation	Abbreviation	Average daily traffic
Health Science	Above ground (AG)	Open-air, Venetian walls on 2 sides	AG1	1903
Thunderbird	Above ground (AG)	Open-air	AG2	1484
Rose Garden	Below ground (BG)	Mechanical ventilation	BG1	970

Sites AG1 and AG2 are above ground open structures; site AG1 has Venetian blind wall on two sides and open-air on the other two sites, site AG2 is open to the air on all sides. Site BG1 is underground and has only one opening at the gate. As such, there are ventilation fans at the corners of each floor inside the parking garage. All the ventilation fans and their pipes are built into the wall and covered with wire mesh at each opening. The fans work intermittently due to their high noise level. Due to this garage being underground, proper ventilation in BG1 is a serious concern and multiple CO detectors are installed at each level by UBC Building operations which are triggered when there are risks for CO poisoning. A simplified schematic of the selected parking garages, as well as the relative positions of RAMPs, are shown in Figure 4.1.

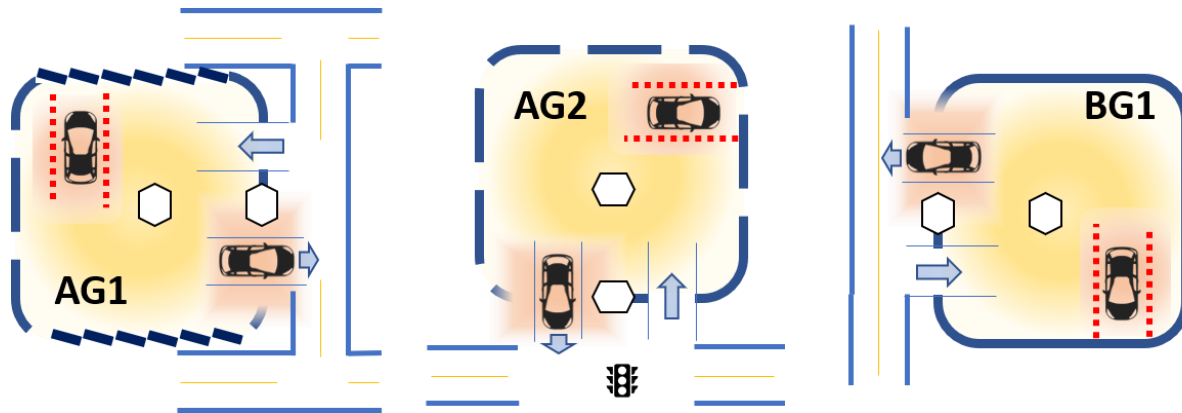


Figure 4.1 Schematic of the parking garages and relative positions of RAMPs, see Table 4.1 for details. The white hexagons represent the RAMP measurement locations. The dash outlines and solid outlines represent an open structure and closed structure, respectively. The angled walls on the top and bottom of AG1 represent the Venetian blind walls on the exterior of the garage. All of the RAMPs are on the same floor except for the RAMPs in Site AG2 in which the RAMP in the center is on the second floor and the distance between the sensors on the same Site is around 50m.

In each parking garage, one RAMP was installed at the gate and one RAMP was installed in the main corridor at the center of each site 1.5-1.8 m above the pavement. Since the parking garages are all multiple level buildings, the sensors at the center are on ground level or between the ground level and next level where the main corridor is a long ramp. There were electricity outlets at the gate of all three garages and at the center of the Site AG2 where RAMPs operated on the external power supply. At Site AG1 center and Site BG1 center, RAMPs were supported by built-in batteries which required a weekly recharge. To keep the continuity of the measurement campaign, two RAMPs were assigned for each of those spots such that there was continuous measurement while one RAMP was charging and thus in total 8 RAMPs were used in this study.

4.2.2 Traffic Patterns at the Sites

Traffic count cameras are installed at the gate of each parking garage and operated by UBC Parking Services. These cameras count the number of vehicles both entering and leaving. Diurnal plots of

the hourly average of the total number of vehicles passing the gate (entering + leaving) are shown in Figure 4.2. Only the vehicle counts on workdays (weekdays, excluding holidays) have been included due to the significant reduction in traffic flow on the weekend and on holidays.

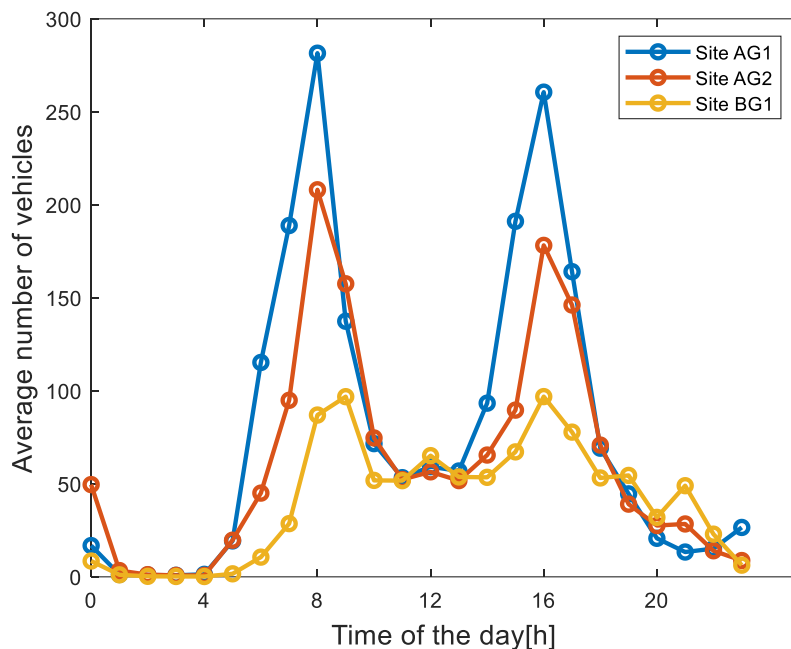


Figure 4.2 Hourly average vehicle counts at the three parking garages in this study.

4.3 Data processing

4.3.1 Background Subtraction

Since the pollutant concentration measured by an air quality monitor is a function of regional background concentration and local sources, to isolate the vehicle emissions signal the background air pollutant concentrations were removed. An algorithm developed by Wang et al. (2018a) was applied to determine and remove this background concentration. This baseline determination algorithm approximates the baseline concentration using 3 input variables including the total concentration, window length and smoothing index. The original algorithm and source code is available in Wang et al. (2018a) but is also described here.

This algorithm determines the baseline concentration by separating the time series into individual windows, identifying the local minimum in each window, and interpolating between the local minima from each window. The output baseline is then smoothed by shifting the window start point and repeating the process. This method can be represented by the following function (represented by f) (Equation 4.1), where the P_{Window} parameter is the window length and P_{Smooth} parameter determines to which extent the background curve is smoothed. P_{Smooth} was assigned to be 3 in this study.

$$C_{\text{Background}} = f(C_{\text{Total}}, P_{\text{Window}}, P_{\text{Smooth}}) \quad \text{Eq. (4.1)}$$

When $P_{\text{Smooth}} = 1$, then the baseline concentrations $C_{\text{Background}}$ is the result of interpolation of minimum values determined in each window of width P_{Window} . This process is repeated 3 times to reduce the bias caused by the length of the window and there will be an offset in start in time by floor ($\frac{P_{\text{Window}}}{3}$). Then the final baseline value is determined as an average (Equation 4.2).

$$C_{\text{Background}} = f(C_{\text{Total}}, P_{\text{Window}}, P_{\text{Smooth}} = 1) = \frac{1}{3} \cdot \sum_{i=1}^3 C_{\text{Background } i} \quad \text{Eq. (4.2)}$$

When $P_{\text{Smooth}} > 1$, the process in above equation will be repeated P_{Smooth} times and the window width will increase by a factor of P_{Window} each time, in which case the window length will be $P_{\text{Window}}, 2P_{\text{Window}} \dots P_{\text{Smooth}} \times P_{\text{Window}}$. The final baseline level is determined as an average as

well (Equation 4.3). Lastly, any value of $C_{\text{Background}}$ will be replaced by the corresponding original concentration if it is greater than the original concentration.

$$C_{\text{Background}} = f(C_{\text{Total}}, P_{\text{Window}}, P_{\text{Smooth}}) = \frac{1}{3 P_{\text{Smooth}}} \cdot \sum_{j=1}^{P_{\text{Smooth}}} \sum_{i=1}^3 C_{\text{Background } i,j} \quad \text{Eq. (4.3)}$$

The P_{Window} was selected by analyzing two factors of the background levels compared with the original concentrations: (1) whether the background level matches the total signal during the quiet hours when no vehicles are entering or exiting the sites and there are few to no vehicles passing the sites; and (2) whether the background level is stable during the peak hours in the afternoon.

For factor 1, the sum of the difference between the total concentration and background concentration on each day was calculated and normalized by the standard deviation of total concentration. The average value of that sum reflects how close the background concentration is to the total concentration during the quiet hours. This result is referred to as ‘Adherence’. The lower the adherence value is, the closer the background concentration is to the total concentration during the quiet hours. For factor 2, the standard deviation of the background concentration during the evening peak hours was calculated for each day and the average value of that standard deviation indicates whether the background concentration could be stable during peak hours. This result is referred to as ‘Stability’. The lower stability is, the more stable the background concentration is during the evening peak hours.

These calculations can be expressed according to Equations (4.4) and (4.5)

$$\text{Adherence (i)} = \sum_{T_1}^{T_n} \frac{C_{\text{Total}}(t) - C_{\text{Background}}(t)}{\text{SD}(C_{\text{Total}}(T_1), C_{\text{Total}}(T_2) \dots C_{\text{Total}}(T_n))} \quad \text{Eq. (4.4)}$$

$$\text{Stability(i)} = \text{SD}(C_{\text{Total}}(T_1'), C_{\text{Total}}(T_2') \dots C_{\text{Total}}(T_n')) \quad \text{Eq. (4.5)}$$

In the equation, *i* corresponds to the day and the two parameters are calculated for each day. T_1, T_n are the beginning and end of the time-period when typically no vehicles are entering or leaving the sites. In this study, $T_1=1\text{AM}$ and $T_2=4\text{AM}$. T_1', T_n' are the beginning and ending of the time-period during afternoon hours when the vehicle counts yield a peak. $T_1'=3\text{PM}$ and $T_2'=7\text{PM}$ in this study.

The determination of the optimal window is shown with CO from the gate of Site AG2. There will be one value of Adherence as well as Stability on each day. To simplify the comparison process, average Adherence value and average stability value has been calculated and shown in Figure 4.3.

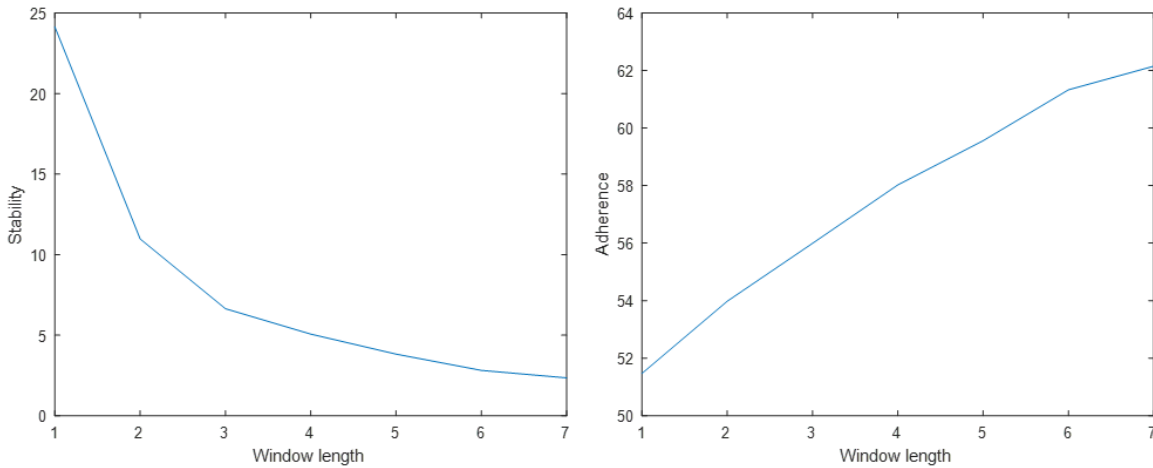


Figure 4.3 Average Stability and Adherence parameters across all campaign days for CO at Site AG2 as a function of window length.

From this analysis, a window length of 5 was chosen across all sites and all pollutants. The influence of window length as well as the smooth index on the background concentrations is shown in Figure 4.4.

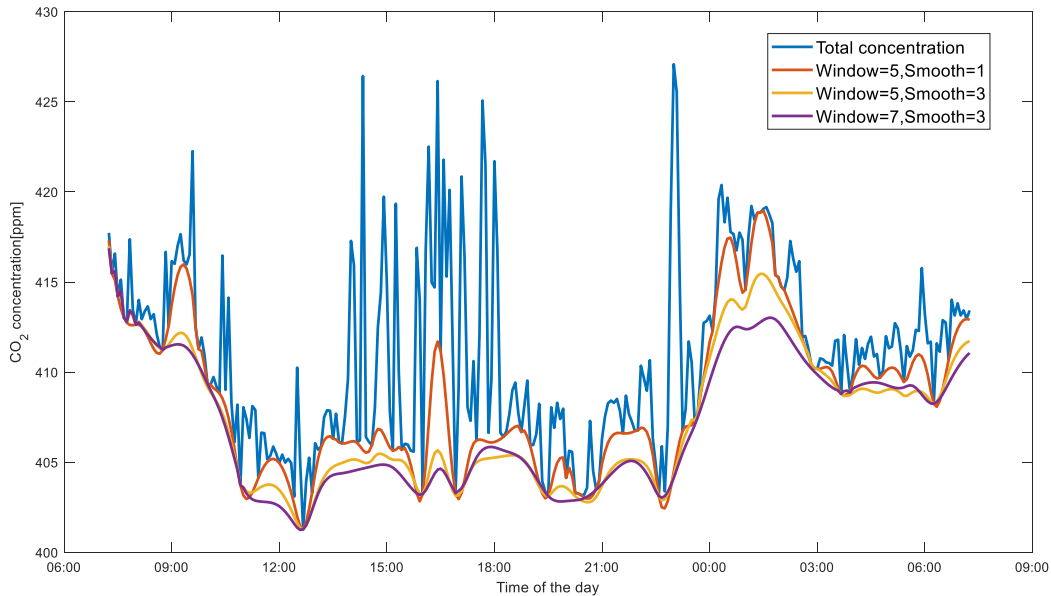


Figure 4.4 The influence of window width and smoothing index on the background concentrations. This is an example of the monitoring data from Site AG2 for around 24 hours.

In this study, a window size of 5 data points (25 minutes) and a smoothing function of 3 (smooth index) was used as the input parameter to develop the baseline concentration of all pollutants and CO₂.

4.3.2 Fuel-based Emission Factors

A fuel-based EF describes the amount of pollutant emitted per unit fuel consumed. Since the time resolution of the data is 5 min, EFs of a group of vehicles (fleet-based EFs) rather than EFs from individual vehicles are calculated. Here, a plume is defined as a concurrent rise and fall in pollutant

and CO₂ concentrations. The plume detection method is detailed in Section 4.3.4. Each plume contains many vehicles and thus the calculated emission factors are more representative of fleet averages.

To calculate the EFs, we used the background-subtracted CO₂ and CO RAMP signals to calculate the amount of carbon released by the combustion which can be converted into a fuel-based estimate based on the carbon content of gasoline (0.86 kg carbon/kg gasoline).

The EF of pollutant Y is calculated according to Eq. (4.6) which is a general equation (Franco et al., 2013; Huang et al., 2016; Pokharel et al., 2002; Wang et al., 2018b, 2018a; Yli-Tuomi et al., 2005).

$$EF_Y = \left(\frac{\Delta[Y] \frac{\text{g}}{\text{m}^3}}{(\Delta[\text{CO}_2] + \Delta[\text{CO}]) \frac{\text{g carbon}}{\text{m}^3}} \right) \times \frac{1000 \text{ g carbon}}{1 \text{ kg carbon}} \times \omega_c \left(\frac{\text{kg carbon}}{\text{kg fuel}} \right) \quad \text{Eq. (4.6)}$$

EF_Y (g/kg fuel) is the fuel-based emission factor of Y while $\Delta[Y]$ (g/m³) is the background-subtracted concentrations of pollutant Y in a plume and $(\Delta[\text{CO}_2] + \Delta[\text{CO}])$ (g carbon/m³) is the increment of carbon in a plume after background subtraction. ω_c is the percentage weight of carbon in the fuel, which is 86.7% for gasoline and 85.7% for diesel (Yli-Tuomi et al., 2005). In this study ω_c was determined to be 86% as it is a routinely used value for the mixed fleet (Wang et al., 2018a, 2018b).

Equation 4.6 provides a simplified version of the calculation. To calculate the EF of pollutant Y (NO, NO₂, CO), we need to convert the unit of the concentration of Y from part per billion (ppb) as measured by the RAMP sensor to g/m³. To do this, we use the molecular weight of pollutant Y and the ideal gas law as shown in Equation 4.7.

$$PV = nRT \quad \text{Eq. (4.7)}$$

Where P is the pressure (Pa), V is the volume of gas (m³), n is the number of moles, R is the ideal gas constant and equal to 8.314J K⁻¹mol⁻¹, T (K) is the absolute temperature and roughly equals 293.15K, standard room temperature.

The concentration of CO and CO₂ also needs to be converted similarly. However, since we are interested in g of carbon in the denominator, we first convert mol of CO and CO₂ to mol of carbon, and then multiple by the molecular weight of carbon. This will be illustrated in the calculation of an EF of NO according to equation 4.8.

$$\begin{aligned}
 & \text{EF}_{\text{NO}} \left(\frac{\text{g}}{\text{kg fuel}} \right) \\
 &= \frac{\left(\Delta[\text{NO}] \times \frac{10^{-9} \text{m}^3 \text{NO}}{\text{m}^3 \text{air}} \times \frac{P}{RT} \left\langle \frac{\text{mol NO}}{\text{m}^3 \text{NO}} \right\rangle \times 30 \left\langle \frac{\text{g NO}}{\text{mol NO}} \right\rangle \right) \times \frac{0.86 \text{ g C}}{\text{g fuel}} \times \frac{1000 \text{ g fuel}}{1 \text{ kg fuel}}}{\left(\Delta[\text{CO}_2] \times \frac{10^{-6} \text{m}^3 \text{CO}_2}{\text{m}^3 \text{air}} \times \frac{P}{RT} \left\langle \frac{\text{mol CO}_2}{\text{m}^3 \text{CO}_2} \right\rangle \times \frac{1 \text{ mol C}}{1 \text{ mol CO}_2} + \Delta[\text{CO}] \times \frac{10^{-9} \text{m}^3 \text{CO}}{\text{m}^3 \text{air}} \times \frac{P}{RT} \left\langle \frac{\text{mol CO}}{\text{m}^3 \text{CO}} \right\rangle \times \frac{1 \text{ mol C}}{1 \text{ mol CO}} \right) \times \frac{12 \text{ g C}}{1 \text{ mol C}}}
 \end{aligned}$$

Eq. (4.8)

The EFs of other pollutants are calculated similarly, with the only replacement being the molecular weight in the numerator of the target pollutant (NO₂ = 46 g/mol; CO = 28 g/mol). In Equation 4.8, units of ppb and ppm are represented on a m³ pollutant per m³ air basis.

4.3.3 Determination of Vehicle Emissions Detection Limit

Due to the noise inherent to low-cost sensor (LCS) signals, there is a need to develop a cut-off value to classify a valid plume from noise. Using the vehicle count data provided by Parking Services, the average background-subtracted concentrations between 1-4 AM were analyzed, removing periods when vehicles entered/exited the parking garages, and used as a representative noise signal. Since the sensors can also be influenced by vehicles passing by on the main road outside the parking garages, we took the 90th percentile value as the noise signal to determine our plume threshold. To be considered for EF calculation, both the pollutant and CO₂ plumes had to exceed this threshold. These cut-off values are reported in Appendix A.

4.3.4 Plume Identifying and Matching

To detect plumes, we first identified every local maximum and minimum in the background-subtracted data set. To be successfully identified as a plume, the following criteria were considered. First, each local maximum (plume peak) needed to exceed the emissions detection limit (Section 4.3.3). Secondly, for each local maximum meeting this requirement, the start and endpoints of the plume were found by identifying the nearest local minima bracketing the peak meeting one or more of the following requirements: 1) local minimum is less than the emissions detection limit; 2) the difference between the peak and minimum concentrations exceeds the emissions detection limit; or 3) the difference between the next furthest peak and the minimum should exceed the emissions detection limit. Local minima criteria number 3 ensures that each local maximum is only included in one plume. The plume identification process is conducted for the pollutants (NO_x, CO, PM_{2.5}) and for CO₂. To calculate the fuel-based EFs, the CO₂ plumes need to be matched with the pollutant plumes. To account for differences in sensor response times,

a small offset of 2 data points in pollutant and CO₂ plume start and endpoints is allowed. This method is illustrated in Figure 4.5.

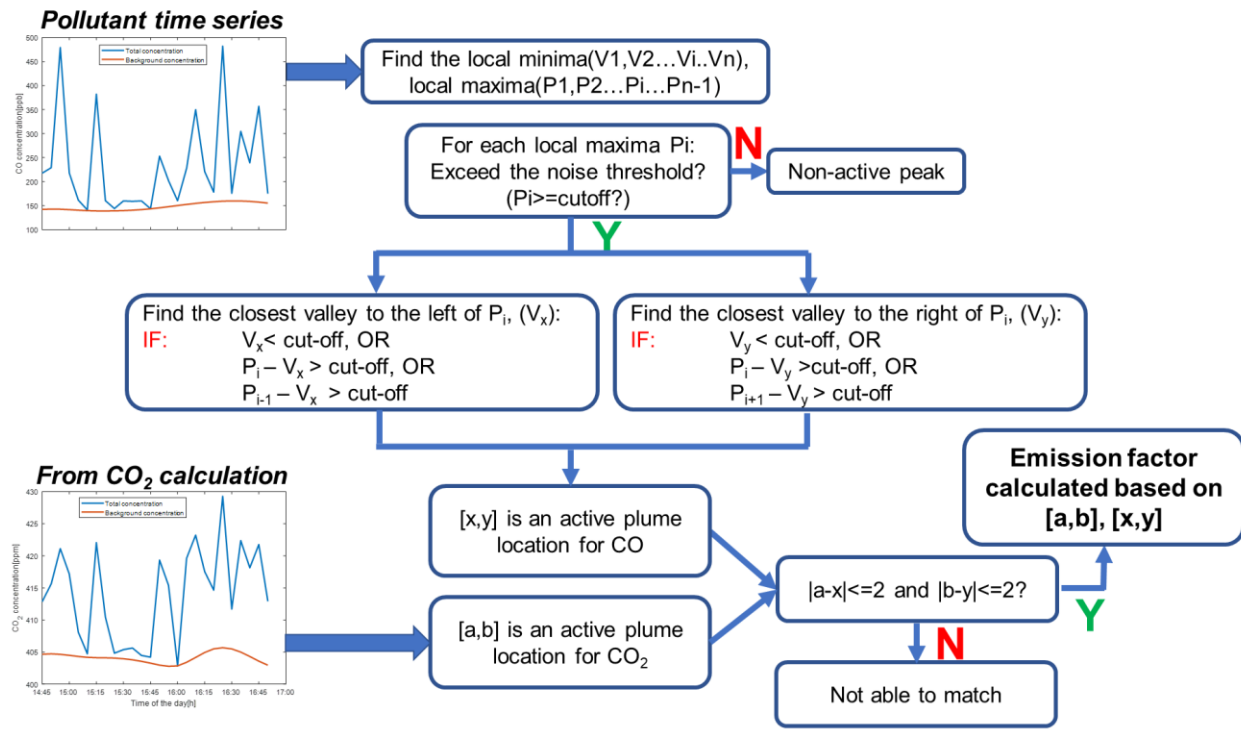


Figure 4.5 Flowchart for identifying start and end times of pollutant and CO₂ plumes. Here [x,y] is the start and end time of a pollutant plume and [a,b] is the start and end time of the CO₂ plume. If plume peaks and local minimums meet specific criteria based on the emissions cut off, and the pollutant and CO₂ plumes are within 2 data points of each other, then an emission factor is calculated.

4.4 Results and Discussion

4.4.1 Diurnal Pollutant Patterns

The weekday diurnal patterns of CO, NO_x, and PM_{2.5} concentration in Site AG2 (Figure 4.6) show that the concentration at the parking garage gate is generally lower than at the center of the garages; this was observed in all three parking garages. For both CO and NO_x, morning and evening rush hour peaks in the center of the garage aligned with the vehicle count peaks from Figure 4.2. Concentrations were generally higher for the evening rush hour peak, likely due to the influence

of cold start emissions. This is discussed in greater detail in Section 4.4.3. PM_{2.5} emissions are less clearly linked with vehicle traffic in the garages.

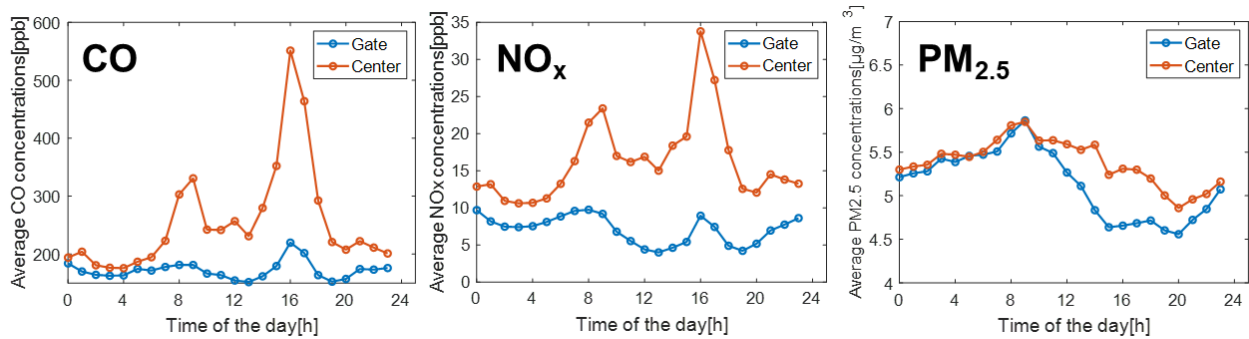


Figure 4.6 Diurnal trend of the hourly average concentrations of targeted gases in Site AG2. The orange curves represent the measurement spot inside the Site AG2, and the blue curves represent the measurement spot at the gate of Site AG2.

At the garage gate, the two rush hour peaks are less distinguishable. At the gate of garage AG2, the sensor is well-exposed to the outside environment and pollutants may be significantly diluted due to wind conditions (Wang et al., 2018a). Furthermore, vehicles pass the Gate sensors more rapidly than the Center sensor, potentially reducing the magnitude of the emissions measured.

The sensors at the center of the garages are more likely exposed to more concentrated plumes due to the slower dispersion limited by the less airflow and ventilation inside the garage. The vertical dispersion of plumes is constrained at each level and the horizontal dispersion is limited by the bearing walls inside the garages. Although AG2 has no exterior walls, there exist multiple bearing walls on each level of Site AG2, which makes the air flowing inside each level lower and slows pollutant plume decay (Leitl and Schatzmann, 2000).

The PM_{2.5} concentration is not well correlated with the vehicle count data, indicating that the fleet entering and exiting the parking facilities is not a major contributor to the fine particles matter mass. Since garages in this study only allow the entry of vehicles smaller than a certain size, the fleet composition was mostly light-duty passenger vehicles predominantly burning gasoline which are less likely to be a significant source of PM_{2.5} compared to diesel vehicles (Li et al., 2018).

There exist air quality standards limiting the concentrations of NO₂, PM_{2.5} outlined in Canadian Ambient Air Quality Standards (CAAQS). The hourly NO₂ concentration limit recommended by CAAQS is 42 ppb and the concentrations of NO₂ are within this range. The recommended upper limit of PM_{2.5} concentration was given as 8.8µg/m³ (8-hour average). The 8-hour average PM_{2.5} concentration in the parking garage is also under this limit. The CO concentration limit is recommended by British Columbia Ambient Air Quality Objectives and the hourly CO concentration limitation recommended is 13,000 ppb which is well above the CO level in the parkade. However, this limit is based on occupational hazards and asphyxiation. Comparing with the regulatory standards of the corresponding pollutants, we found the concentration levels are mostly below the values outlined by Canadian standards and B.C. standards.

4.4.2 Overall Fleet-based Emission Factors

Emission factors were calculated for CO, NO_x and PM_{2.5} and compared with previously published studies of real-world, gasoline vehicle EFs using reference-grade instruments (Table 4.2). As we used the plume-based approach, fuel-based EFs were directly calculated. However, to expand our ability to compare to published studies, we also converted published distance-based EFs to approximate fuel-based emission factors using an average fuel economy of 9 L/100 km (Evans et

al., 2019) and a fuel density of 0.755 kg/L. There is some uncertainty within this conversion since the average fuel economy we used was estimated from a recent multi-year study on a heavily trafficked road in Vancouver; however, the fuel economy normally varies within a stable range (Tsokolis et al., 2020), which supports this conversion. Our reported average EFs were calculated excluding EFs from the center of Site BG1. Since the airflow at the center of BG1 was noticeably lower than other measurement spots (poor ventilation), pollutants were stagnant and not rapidly decaying, making background subtraction and plume identification highly uncertain.

Table 4.2 Comparing the average emission factors developed in this study with previous work (light-duty vehicles only). To convert fuel-based emission factors into distance-based emission factors, we used an average fuel economy of 9L/100 km and a fuel density of 0.755 kg/L. Our EFs are expressed as average +/- a 95% confidence interval (The emission factors developed from Site BG1 center were not included) and the uncertainty of the instruments after calibration is not included.

Pollutant	This study		Other studies	Units	Studies
	All	Morning entering only			
CO	18.5 ± 0.4	14.5 ± 0.6	10.3 – 26.4	g kg-fuel ⁻¹	1, 2, 3, 4, 5
NO _x	1.84 ± 0.03	1.78 ± 0.06	1.2 – 3.2	g kg-fuel ⁻¹	1, 2, 3, 4, 5, 6, 7
PM _{2.5}	0.22 ± 0.03	0.27 ± 0.03	0.15 – 1.1	g kg-fuel ⁻¹	8, 9, 10

¹Dallmann et al. (2013), ²Wang et al., (2015), ³Bishop and Stedman (2014), ⁴Larson et al. (2017), ⁵May et al. (2014), ⁶Hudda et al. (2013), ⁷Li et al. (2020), ⁸Lawrence et al. (2016), ⁹Krecl et al. (2018), ¹⁰Abu-Allaban et al. (2003)

Compared to other studies, our calculated EFs were similar to those from the published literature. The average published CO EF was approximately 17.9 g kg-fuel⁻¹, in line with what was observed here. While the upper range of the NO_x emission factors reported is 3.2 g kg-fuel⁻¹, the average across the seven studies was approximately 2.2 g kg-fuel⁻¹, higher than the 1.8 g kg-fuel⁻¹ reported here. However, this may be a function of changing fleet characteristics due to tightening regulations over time; a recent study in Pittsburgh, PA determined a NO_x emission factor of 1.2 g kg-fuel⁻¹ (Li et al., 2020). The most uncertainty is in the PM_{2.5} emission factors, as there is limited

published data available for gasoline vehicles and a wide range of published emission factors depending on the source of the PM including brake wear, tire wear and tailpipe PM_{2.5}.

4.4.3 Determination of the Relative Importance of Cold Start

To compare the EFs of cold start with normal operations, plumes from each measurement spot have been classified into several groups by the time of the plume and the direction of most of the vehicles in the plume (entering vs. leaving). Considering that there is no clear and consistent definition of the timing, engine conditions and vehicle conditions for cold start phase in published literature and that we are not able to isolate the cold start phase absolutely in this fleet-based research, the impacts we are measuring we refer to as cold start could be considered a “pseudo” cold start.

Here we distinguish between two conditions: 1) vehicles entering the garage in the morning (expected to be fully warmed up) and 2) vehicles leaving the garage in the evening (potential influence of cold start). In condition 1, we isolated all plumes where >75% of the vehicle traffic was entering the garage between the hours of 6-10 AM. In condition 2, we isolated all plumes where >75% of the vehicles were leaving the garage between the hours of 4-8 PM. As part of this plume classification, we also required at least 5 vehicles per plume. We expect plumes classified as part of condition 2 to represent cold-start emissions since it has been shown that these effects persist for the first few miles of the trip due to the low temperature of the three-way catalyst and coolant, as well as less efficient combustion caused by the lower air-to-fuel ratio during the cold start phase (Badshah et al., 2016; Ligterink, 2016; Reiter and Kockelman, 2016).

In this study, we compared the impacts of cold start on CO and NO_x EFs. We hypothesize that the PM_{2.5} EFs are mostly brake and tire-wear particles which are much larger and fell within the detecting range of our instruments. We expect the primary influence of cold start on PM to be within the ultrafine particle size range (<100 nm), which is beyond the range of detection for our sensors. The resulting time-separated EFs of CO and NO_x are shown in Figure 4.7.

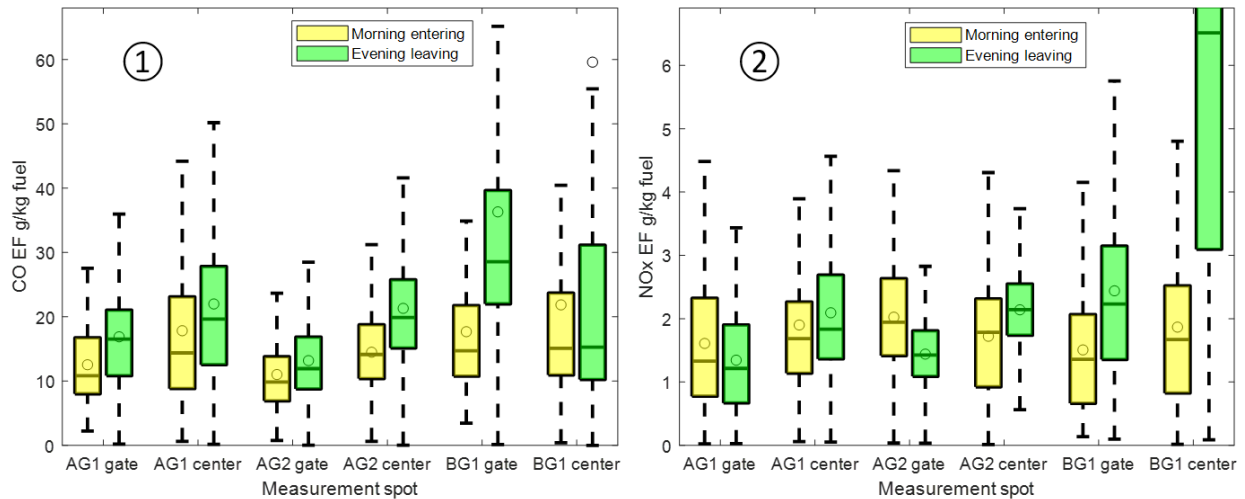


Figure 4.7 Comparison of Emission factors (1: CO; 2: NO_x) between morning entering vehicles and evening leaving vehicles from 6 measurement spots of 3 sites. For the box plots, whiskers are 10th and 90th percentile, box edges are 25th and 75th percentiles, the line is the median, and the circle markers in blue are the average.

In general, the morning EFs (yellow bars) across the different locations and sites are similar. In the evening (green bars), most EFs are similar across locations except for site BG1 center. The airflow and ventilation at that measurement spot is limited due to the indoor and underground environment, thus there exists more uncertainty in the calculation of EFs of which one of the assumptions is the same dilution rate for pollutants and CO₂. We believe that the accumulation of pollution throughout the day at the center of site BG1 yielded evening EFs inconsistent with the other sites.

The CO EFs in the evening leaving plumes (Figure 4.7, green) tended to be higher than the morning entering plumes (Figure 4.7, yellow), though the increase at the gate of Site AG2, the most well-ventilated site, is the smallest. This shows that the LCS system is capable of measuring some cold start emissions and that effect is still detectable when the vehicles are passing the gates. Theoretically, CO engine-out emissions are high during cold start period because of the lower air-to-fuel ratio (Dardiotis et al., 2013; Franco et al., 2013; Khan and Frey, 2018; Suarez-bertoa and Astorga, 2018; Zhu et al., 2016), which is a common control strategy against the low gasification rate of fuel to provide enough combustible charge during low-temperature operation. CO is a common product of incomplete combustion. Simultaneously, the three-way catalyst (TWC) also needs approximately 2 minutes to reach its light-off temperature (Bielaczyc et al., 2014; Reiter and Kockelman, 2016). The conversion efficiency of the TWC below the light-off temperature is significantly lower and yields higher tail-pipe CO emissions.

There exist more specific reasons to explain the increased evening emissions for individual vehicles since the characteristics of the engine and the TWC, the cold start control strategies, and the vehicle emission standards vary widely. Though we are not able to confirm every vehicle would have an increased CO EF during the cold start phase, the result reflects the fleet exhibiting higher CO emissions at the start of a trip by approximately 52%. Though previous studies mostly quantify the concentration of pollution rather than EFs during the cold start, an estimated increase in CO EF of 50% to 100% compared with normal operating conditions is expected assuming the emission of CO₂ is constant (Favez et al., 2009). The smaller increase in our study is not unexpected since the plumes we measured cannot be guaranteed to be the first phase of the cold start when the emission rate is highest (Suarez-bertoa and Astorga, 2018).

The NO_x EFs had a slightly increasing trend when comparing morning entering and evening leaving. In this study, we observed NO_x EFs approximately 9% higher in the leaving evening plumes, however, it is uncertain how long that effects persist since we don't see an increase in the evening at the gate of sites AG1 and AG2. Previous research has shown uncertain results about the impact of cold start on fuel-based NO_x EFs of individual vehicles (Bielaczyc et al., 2014; Cédric et al., 2016; Dardiotis et al., 2013; He et al., 2018; Khan and Frey, 2018; Yao et al., 2009). NO_x is produced by the reaction between components of air, rather than the fuel, which means the connection between fuel and NO_x is indirect. The low air-to-fuel ratio at cold start is presumably contributing to less engine-out NO_x but the low-efficiency of the TWC below light-off temperature would lead to more tailpipe NO_x emissions. Previous research indicated that cold start NO_x emission has complex trends determined by the after-treatment configurations as well as cold start control strategies (Ligterink, 2016; Suarez-bertoa and Astorga, 2018; Yao et al., 2009). The slight increase of NO_x emission factor in the morning at the Site AG1 gate might be partially due to that complex uncertainty, however, the location of Site AG1 and also the gate sampling location may also have affected the results; the AG1 gate sensor is approximately 5 meters from an intersection controlled by stop signs where vehicles would undergo a series of transient operation modes and potentially produce more emissions (Qiao et al., 2005). The slightly higher EFs may come from the plumes from the intersection or the road outside the gate.

The AG2 garage gate sensor is roughly 3 meters from an intersection controlled by traffic lights on a major road leading to the campus. Heavy-duty vehicles, including recycling trucks and delivery trucks, going past and idling at the intersection could have significant impacts on the NO_x levels detected by the AG2 gate sensor due to the significantly higher levels of NO_x emissions

from heavy-duty vehicles as well as the long decaying time of NO_x plumes (Karner et al., 2010; Quiros et al., 2018). These campus HDVs are mostly active in the morning. Thus, we are not able to conclusively determine the impact of cold start on NO_x EFs.

4.4.4 Assessing the relative contribution of high emitters

The relative contribution of high emitters was assessed based using the morning-entering EFs (Figure 4.8, left side) and for both morning-entering and evening leaving EFs (Figure 4.8, right side). Due to the aforementioned ventilation concerns, the EFs from Site BG1 center were not included. As has been mentioned in previous studies, the fuel economy does not change significantly (Tsokolis et al., 2020) which allows us to consider the fuel consumption of each plume as generally consistent. The amount of pollutant (AoP) emitted during each plume is then calculated with the corresponding emission factor and consistent fuel consumption.

Here we use CO as an example to illustrate this process and EF_i is the EF of one CO plume (plume i). Since the mixing and diluting of exhaust, as well as the formation of the plume, has not been characterized, we assume there is a signature emitter that causes the emission of that plume. The fuel economy of LDVs are mostly constant and F here stands for the fuel economy of a typical LDV, with the unit being L/100km and the distance a vehicle travels while leaving the parking garage is another constant value D with the unit being km. The calculation of AoP of plume i is given as Eq. (4.9).

$$AoP_i = EF_i \times F \times D \quad \text{Eq. (4.9)}$$

The AoP_i is then ranked from the smallest to the greatest. Total amount of emission is calculated as $AoP_{Total} = \sum AoP_i$. The contribution of the top 5% emitters is calculated as Eq. (4.10):

$$P_{Top\ 5\%} = \frac{\sum_{95^{th}\ percentile\ AoP_i}^{greatest\ AoP_i} AoP_i}{AoP_{Total}} \quad \text{Eq. (4.10)}$$

Similarly, the contribution of the top 10%, 25% emitters is calculated. Once that calculation is repeated for a continuous percentile of emitters, we can plot the cumulative distribution as shown on the right of Figure 4.8.

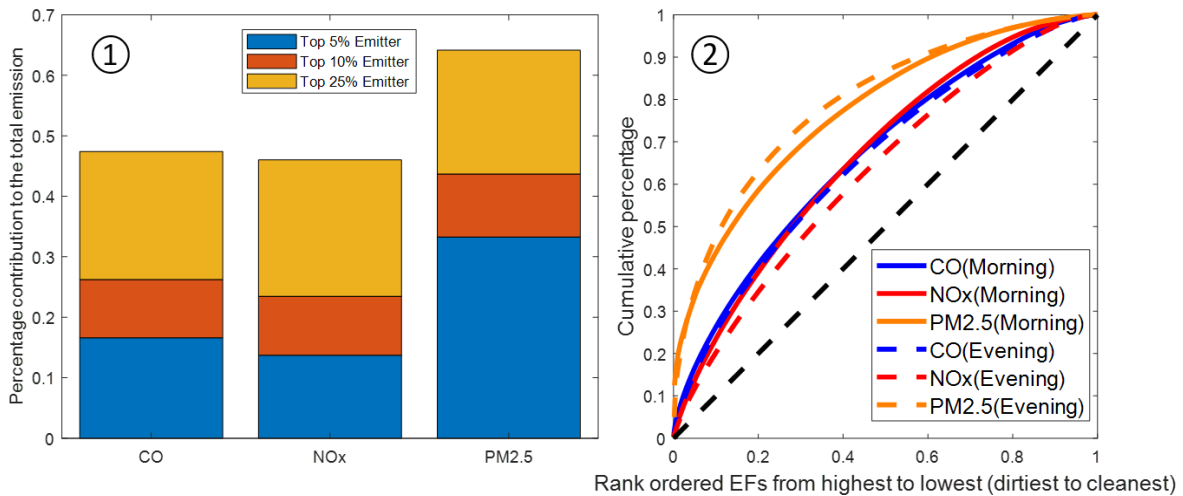


Figure 4.8 Relative contribution of heavy emitters. Side 1 shows the morning entering EFs, and Side 2 shows both morning entering and evening leaving EFs (excluding site BG1 center).

As is shown in Figure 4.8, high emitters disproportionately contribute to fleet emissions. For example, the top 25% emitters account for nearly 50% of the total CO and NO emissions. Similar findings were presented in previous studies (Wang et al., 2015). The greater contribution from high emitters indicates the majority of the fleet is having a lower emission factor and there exists

a possibility to reduce total emission significantly by optimizing the emissions of a smaller number of vehicles or targeting these vehicles for removal.

By plotting this data on a cumulative curve (Figure 4.8, right side) we can see this effect further. If the total emissions are distributed proportionally (each plume contributes equally to total emissions), the cumulative percentage curve should follow the 1:1 line. Here, the curves bend upwards, illustrating the relative contribution of high emitters. This trend doesn't change significantly when including the cold, evening-leaving EFs, which indicates both regular emitters and high emitters' EFs changed in a similar way when the cold start phase is included. For CO and NO_x, both high emitters and regular emitters have a similar increase when we include the cold-start phase.

4.5 Errors and uncertainty

4.5.1 Uncertainty of the instruments

There have been multiple uncertainties that remain in this method. Firstly, the errors of the instruments after the calibration is not included in the calculation of the EF in this chapter. Also, the error generated by relocating the instruments from the calibration sites to the parking garages exist but is not certain. With more progress in sensor calibration and additional validation at the parking garages, the uncertainty with the instruments could be further quantified and reduced. Here the thesis sought to replicate published emission factor approaches, which tend to not propagate instrument uncertainty.

4.5.2 Uncertainty of the methods

There exists uncertainty within the methods, including determining the background concentrations, determining the noise cut-off value, detecting the plumes, matching the plumes and calculating the EF. It's uncertain whether the background concentration is accurate due to the lack of actual measurement of the background level with a nearby background station. While finding out the noise cut-off concentration, it's uncertain the percentage of noise being filtered out in this way and how much real signal is removed as noise. When we determine a plume from the time series, the error rate is not certain. Especially for the EF carbon balance calculation, due to the time resolution of the data, the amount of pollutants and CO₂ is a rough estimation. Overall, the EF developed in this study may not reflect the real EF of the fleet since there is very limited published studies to confirm or compare against and we did not include the uncertainty in the EFs as calculated by low-cost sensors. The uncertainty within the methods is especially challenging to quantify since the methods are applied for the first time to low-cost sensing studies and the uncertainty needs more future work to be fully quantified. However, the main target of this work is to answer the question: Can we use low-cost sensors to measure vehicle emissions. The value of this work is that a comprehensive method applying low-cost sensors to vehicle emissions measurement has been proposed and tested. The quantification and reduction of uncertainty is important but would not be the most important target of this work and will be addressed in future studies.

4.6 Conclusions

In this chapter, we found the concentrations of CO and NO_x correlate with the vehicle traffic count; the peaks in the concentrations of CO and NO_x correspond to peaks in the vehicle count data.

Meanwhile, we found the concentrations of pollutants and CO₂ measured in the center are generally higher than those measured at the gate. After developing a background subtraction algorithm and converting the pollutant signal to emission factors, we found that emission factors of CO, NO_x and PM_{2.5} developed in this study aligned well with previous studies using regulatory instruments. By isolating the morning-entering plumes from the evening-leaving plumes the impact of pseudo-cold start was assessed. We found that the cold start phase has more significant impacts on the emission of CO than that of NO_x. Also, the high emitters are found to have disproportionately high contribution to the total emissions which suggests that upgrading or scrapping a small fraction of vehicles may improve emissions greatly.

Chapter 5: Conclusions and Future work

5.1 Overall Conclusions

Low-cost sensors are a promising option for measuring vehicle emissions as well as calculating fleet-based EFs. As sensors and data analysis methods continue to evolve, low-cost sensors could be deployed on a large scale to support real-time air quality monitoring and the assessment of fleet characteristics under a wide range of operating conditions. This large quantity of high-resolution data from a broad air quality sensor network would strengthen environmental policy decisions and assessment of policy impacts.

Within our study, CO and NO_x concentrations increase significantly during peak hours, especially inside the parking garage. Pedestrians walking to their cars will have more exposure to vehicle emissions during that time. Given the very high concentrations in the BG1 garage, fans and other methods increasing ventilation should be enhanced to minimize the risks and drivers should be encouraged to use the parking garages out of peak hours when possible.

According to our real-world measurement results, most light-duty vehicles had higher fuel-based CO, NO_x emission factors during the pseudo-cold-start phase when leaving the garage in the evening. The increase in CO EF is much more significant than that of NO_x, which indicates reducing CO emissions during cold-start should still be a priority. This could be achieved by optimizing the control strategies during cold start as well as improving the conversion efficiency of the TWC at cold temperatures.

5.2 Revisiting the Objectives

5.2.1 Objective 1: Calibrating low-cost sensors in a traffic-rich environment

By applying the calibration algorithms developed previously to a sensor collocation at a near-road regulatory monitoring station in partnership with Metro Vancouver, a hybrid machine-learning and multiple linear regression model was tuned and validated. The calibration performance was similar to previously published studies. Based on the calculated emission factors and observed concentrations in the parking garages, the calibration algorithm had good transferability to the parking garage environment.

5.2.2 Objective 2: Developing a method for determining fleet-based vehicle emission factors with low-cost sensor data

In this study, an advanced background subtraction algorithm and noise limit determination method was developed and testing, using vehicle counting data collected by UBC Parking Services as a built-in validation. A plume identification algorithm was developed and applied to the background-subtracted data and converted into a fuel-based emission factor using the carbon balance method. A protocol for determining minimum plume magnitude for consideration was also determined. These thresholds can serve as guidelines for future deployments.

5.2.3 Objective 3: Comparing the calculated emission factors to those in the published literature

The emission factors of NO_x , CO, and $\text{PM}_{2.5}$ calculated here were compared to ten published studies. The emissions factors calculated with the low-cost sensing system were in-line with those from published studies using reference-grade instruments orders of magnitude more expensive.

This preliminary assessment suggests that low-cost sensors are promising tools for the measurement of vehicle emission factors in urban environments.

5.2.4 Objective 4: Assessing the relative importance of cold start on vehicle emissions

By categorizing emission factor plumes as morning-entering or evening-leaving within certain time windows, the impacts of the pseudo-cold start were assessed, assuming that vehicles leaving the parking garages in the evening have been parked for most of the business day and the engines are relatively colder. We found that most light-duty vehicles had higher fuel-based CO and NO_x emission factors during the evening. The increase in CO emission factor (approximately 50%) is much more significant and common than that of NO_x (approximately 10%), which indicates reducing CO emissions during cold start should still be of priority. The PM_{2.5} emission factor was not significantly impacted by the cold start phase in this study.

5.3 Limitations of This Work and Challenges of the Field

5.3.1 The limitation of our study exists in several aspects

1. There is limited validation of the background concentration of pollutants and CO₂, due to a lack of reference-grade instruments deployed at any nearby regional background location.
2. There is a lack of laboratory testing of vehicle fuel-based emission factors during the cold start phase in previous studies as well as in our study. Whether the real-world results would match the laboratory results remains unknown.

3. We did not quantify the influence from the vehicles passing the sensors on the roads parallel to the sites which would also cause uncertainty. Ideally, sensors would be placed in the parking garages and on the parallel road to subtract this effect.
4. There is a lack of validation of the calibration after relocating to the parking facilities from the roadside regulatory collocation site. As was mentioned in Chapter 2, the location will influence the performance of the low-cost sensors if the primary components of pollutants are not identical. There is a need to do a site-based validation to prove the calibration model is valid after being moved to the real sites. However, since both methods were dominated by traffic, we expect these effects to be small.
5. Detailed vehicle statistics beyond vehicle count were missing. As such, there is some uncertainty about the percentage of diesel vehicles and old vehicles. Our results assume that there is no systemic schedule of when these special vehicles appear and that they are evenly distributed in a day. However, further validation may be needed to remove the possible influence of the emission patterns from the special high emitters.

5.3.2 Challenges in the field more broadly

1. There is an ongoing challenge in collecting data from a large fleet. Based on the literature, most of the studies have compared the emission factors between the cold-start phase and normal operation from individual vehicles. That could be due to the high cost of the instruments as well as the complex procedures installing the instruments on the testing

vehicle. Though we have low-cost sensors, tests based on reference-grade instruments are still required for comparison and validation.

2. There is a challenge in defining the cold start phase. Previous pieces of literature have had different definitions of the length of that transient phase which makes it hard to make a practical comparison between cold start and normal operations since the cold start emission change quickly with engine temperature rising. There should be a systematic definition of cold start, for example, the temperature of the engine, catalyst converter, etc. In acknowledgement of this issue, we refer to our cold start impacts as “pseudo” cold start.
3. There is a challenge in finding the individual contribution out of a mixed plume with multiple vehicles. Previous research could find out the individual plume either by conducting the campaign without other vehicles, for example, at night or by chasing measurement or by using fast instrumentation, which is less subject to the interference from vehicles nearby. Current low-cost sensors are not responsive enough to detect individual vehicles and as such, this is an area needing further development.
4. There is a challenge in conducting roadside studies with low-cost sensors. The low-cost sensors are not as sensitive as traditional instruments. The roadside environment is not as pollutant intensive as parking garages and the dilution of pollutants is also faster which makes the signal much less intense and creates further challenges separating the signal from the noise. Also, the environmental conditions such as the wind will have more impact on the results, for instance, the emission measured downwind from the source is higher

than at an upwind location. Environmental conditions need to be documented and taken into account.

5.4 Implications for stakeholders and future research directions

5.4.1 Implications for stakeholders

From this study, there are a few recommendations for the stakeholders further reduce vehicle emissions and exposure.

1. Parking operators: The real-time emissions of vehicles could be reported to the public to increase public awareness of vehicle emissions and environmental impacts. More ventilation machinery could also be installed, especially at the underground parking garages to reduce the health hazards of the accumulated exhaust.
2. Car owners: Discourage private vehicle use and take public transportation instead to reduce exposure when in the garages. Owners should be encouraged to maintain their vehicles frequently to ensure TWC and other after-treatment devices can work with high efficiency.
3. Vehicle manufacturers: Optimize the after-treatment system as well as control strategies to reduce emissions during the cold-start phase. The vehicle should also be able to indicate the working conditions of the after-treatment system and inform the driver once any part of the after-treatment system needs to be replaced.
4. Policymakers: Continue to support policies that motivate the public to switch to clean technologies, to reduce the impact of combustion emissions. Enhance vehicle emissions

testing procedures to use real-world based estimates to better capture vehicle emissions variability and reinstate “cash for clunkers” programs to remove old, high emitting vehicles from the roadway.

5.4.2 Future research directions

1. Further testing and validation of the calibration results is recommended going forward. Based on previous research, very few studies validate their calibration model and results at different locations. Previously, we validated the calibration model with the testing data collected at the same place and there exists some uncertainty of whether the model will hold after the relocation. Going forward, a new calibration model based on machine learning could be built after the collocation campaign, followed by a validation near-road campaign at a different place, preferably on the UBC Vancouver campus, with a mobile lab being the reference. The results of the near-road campaign could be compared with the mobile lab data to see the error rate of the calibration model.
2. Testing the capability of low-cost sensing packages in a more general scenario, for instance, the next step could be installing RAMPs by the side of major roads on the UBC Vancouver campus, with a vehicle counting device helping determine if vehicles are passing by. Emission factor calculations could also be conducted at the Metro Vancouver Clark Drive station. The purpose of this test is to see the potential of monitoring vehicle emissions from a less emission-intensive location with less traffic density while vehicles are more likely to be operating under normal speed. Also, this will help explore the relationship between the intersection and emissions. Based on the new results, we could

make conclusive statements about the suitability of low-cost sensors like the RAMPs for measuring vehicle emission factors. Sampling at a near-road location would also better replicate the sampling conditions of most of the previous roadside / remote sensing studies.

3. After the campaign on UBC Vancouver campus, we will need to further evaluate the potential of low-cost sensors to quantify the emission factors in more complex scenarios, for example, we may deploy a larger number of RAMPs near various roads in Vancouver and evaluate the emission factors of the vehicle fleets in the city and even western Canada. Using a mobile lab installed with reference-grade instruments and moving around different locations will help with calibration as well as evaluation of the emission factors. Chasing measurement could also be applied to measure specific vehicles to bridge the emission factors of individual vehicles and vehicle fleets. The target is to have a thorough comparison between different measurement methods, instruments to fully utilize the potential of low-cost sensors in urban air quality monitoring and emissions evaluation.

Bibliography

- Abu-Allaban, M., Gillies, J.A., Gertler, A.W., Clayton, R., Proffitt, D., 2003. Tailpipe, resuspended road dust, and brake-wear emission factors from on-road vehicles, in: Atmospheric Environment. pp. 5283–5293. <https://doi.org/10.1016/j.atmosenv.2003.05.005>
- Alföldy, B., Giechaskiel, B., Hofmann, W., Drossinos, Y., 2009. Size-distribution dependent lung deposition of diesel exhaust particles. *J. Aerosol Sci.* 40, 652–663. <https://doi.org/10.1016/j.jaerosci.2009.04.009>
- Anenberg, S., Miller, J., Henze, D., Minjares, R., 2019. A global snapshot of the air pollution-related health impacts of transportation sector emissions in 2010 and 2015. *Int. Counc. Clean Transp.* 55.
- Austin, C.C., Goyer, N., 2006. Cross-sensitivities of electrochemical detectors used to monitor worker exposures to airborne contaminants : False positive responses in the absence of target analytes. <https://doi.org/10.1039/b510084d>
- Badshah, H., Kittelson, D., Northrop, W., 2016. Particle Emissions from Light-Duty Vehicles during Cold-Cold Start. *SAE Int. J. Engines* 9, 1775–1785. <https://doi.org/10.4271/2016-01-0997>
- Bento, A., Freedman, M., Lang, C., 2015. Who benefits from environmental regulation? evidence from the clean air act amendments 97, 610–622. <https://doi.org/10.1162/REST>
- Bielaczyc, P., Szczotka, A., Woodburn, J., 2014. Cold start emissions of spark-ignition engines at low ambient temperatures as an air quality risk. *Arch. Environ. Prot.* 40, 86–100. <https://doi.org/10.2478/aep-2014-0026>
- Bielaczyc, P., Woodburn, J., Szczotka, A., 2020. Exhaust Emissions of Gaseous and Solid

Pollutants Measured over the NEDC , FTP-75 and WLTC Chassis Dynamometer Driving Cycles. <https://doi.org/10.4271/2016-01-1008>. Copyright

Bishop, G.A., Stedman, D.H., 2014. The recession of 2008 and its impact on light-duty vehicle emissions in three western United States cities. *Environ. Sci. Technol.* 48, 14822–14827. <https://doi.org/10.1021/es5043518>

Boere, A.J.F., Fokkens, P.F.H., Leseman, D.L.A.C., Augsborg, K., Cassee, F.R., Bokkers, B.G.H., Sachse, H., Reijnders, J.J.E., 2019. Inhalation toxicity profiles of particulate matter : a comparison between brake wear with other sources of emission. *Inhal. Toxicol.* 31, 89–98. <https://doi.org/10.1080/08958378.2019.1606365>

Bonatesta, F., Chiappetta, E., La Rocca, a., 2014. Part-load particulate matter from a GDI engine and the connection with combustion characteristics. *Appl. Energy* 124, 366–376. <https://doi.org/10.1016/j.apenergy.2014.03.030>

Brauer, M., Freedman, G., Frostad, J., van Donkelaar, A., Martin, R. V, Dentener, F., van Dingenen, R., Estep, K., Amini, H., Apte, J.S., Balakrishnan, K., Barregard, L., Broday, D., Feigin, V., Ghosh, S., Hopke, P.K., Knibbs, L.D., Kokubo, Y., Liu, Y., Ma, S., Morawska, L., Texcalac Sangrador, J.L., Shaddick, G., Anderson, H.R., Vos, T., Forouzanfar, M.H., Burnett, R.T., Cohen, A., 2016. Ambient air pollution exposure estimation for the global burden of disease 2013. *Environ. Sci. Technol.* 50, 79–88. <https://doi.org/10.1021/acs.est.5b03709>

Breuer, M.A., Burgard, D.A., 2019. Bridge-based remote sensing of NO_x emissions from locomotives. *Atmos. Environ.* 198, 77–82. <https://doi.org/10.1016/j.atmosenv.2018.10.046>

Budde, M., Schwarz, A.D., Müller, T., Laquai, B., Dittler, A., Beigl, M., 2018. Potential and Limitations of the Low-Cost SDS011 Particle Sensor for Monitoring Urban Air Quality

- Potential and Limitations of the Low-Cost SDS011 Particle Sensor for Monitoring Urban Air Quality. <https://doi.org/10.14644/dust.2018.002>
- Burgard, D.A., Bria, C.R.M., Berenbeim, J.A., 2011. Remote sensing of emissions from in-use small engine marine vessels. *Environ. Sci. Technol.* 45, 2894–2901. <https://doi.org/10.1021/es1027162>
- Campbell-Lendrum, D., Prüss-Ustün, A., 2019. Climate change, air pollution and noncommunicable diseases. *Bull. World Health Organ.* <https://doi.org/10.2471/BLT.18.224295>
- Camuffo, D., della Valle, A., Becherini, F., 2018. A critical analysis of one standard and five methods to monitor surface wetness and time-of-wetness. *Theor. Appl. Climatol.* 132, 1143–1151. <https://doi.org/10.1007/s00704-017-2167-9>
- Castell, N., Dauge, F.R., Schneider, P., Vogt, M., Lerner, U., Fishbain, B., Broday, D., Bartonova, A., 2017. Can commercial low-cost sensor platforms contribute to air quality monitoring and exposure estimates? *Environ. Int.* 99, 293–302. <https://doi.org/10.1016/j.envint.2016.12.007>
- Cédric, L., Goriaux, M., Tassel, P., Perret, P., André, M., Liu, Y., 2016. Impact of aftertreatment device and driving conditions on black carbon , ultrafine particle and NO_x emissions for Euro 5 Diesel and gasoline vehicles. *Transp. Res. Procedia* 14, 3079–3088. <https://doi.org/10.1016/j.trpro.2016.05.454>
- Chang, Y., Yang, W., Zhao, D., 2018. Energy Efficiency and Emission Testing for Connected and Automated Vehicles Using Real-World Driving Data. <https://doi.org/arXiv:1805.07643v2>
- Chong, C., Kumar, S.P., Member, S., 2003. *Sensor Networks : Evolution , Opportunities , and Challenges* 91.
- Clemitchaw, K., 2010. *Technology A Review of Instrumentation and Measurement Techniques*

- for Ground-Based and Airborne Field Studies of Gas-Phase Tropospheric Chemistry A Review of Instrumentation and Measurement Techniques for Ground-Based and Airborne Field Studies of Gas-Pha 3389. <https://doi.org/10.1080/10643380490265117>
- Çolak, S., Lima, A., González, M.C., 2016. Understanding congested travel in urban areas. *Nat. Commun.* 7. <https://doi.org/10.1038/ncomms10793>
- Creutzenberg, O., 2012. Biological interactions and toxicity of nanomaterials in the respiratory tract and various approaches of aerosol generation for toxicity testing. *Arch. Toxicol.* 86, 1117–1122. <https://doi.org/10.1007/s00204-012-0833-3>
- Cross, E.S., Williams, L.R., Lewis, D.K., Magoon, G.R., Onasch, T.B., Kaminsky, M.L., Worsnop, D.R., Jayne, J.T., 2017. Use of electrochemical sensors for measurement of air pollution: Correcting interference response and validating measurements. *Atmos. Meas. Tech.* 10, 3575–3588. <https://doi.org/10.5194/amt-10-3575-2017>
- Dallmann, T.R., Kirchstetter, T.W., DeMartini, S.J., Harley, R.A., 2013. Quantifying on-road emissions from gasoline-powered motor vehicles: accounting for the presence of medium- and heavy-duty diesel trucks. *Environ. Sci. Technol.* 47, 13873–13881. <https://doi.org/10.1021/es402875u>
- Dardiotis, C., Martini, G., Marotta, A., Manfredi, U., 2013. Low-temperature cold-start gaseous emissions of late technology passenger cars. *Appl. Energy* 111, 468–478. <https://doi.org/10.1016/j.apenergy.2013.04.093>
- Dario, C., 2019. A method to obtain precise determinations of relative humidity using thin film capacitive sensors under normal or extreme humidity conditions. *J. Cult. Herit.* 37, 166–169. <https://doi.org/10.1016/j.culher.2018.11.003>
- De Vito, S., Piga, M., Martinotto, L., Di Francia, G., 2009. CO, NO₂ and NO_x urban pollution

- monitoring with on-field calibrated electronic nose by automatic bayesian regularization. *Sensors Actuators, B Chem.* 143, 182–191. <https://doi.org/10.1016/j.snb.2009.08.041>
- Dedoussi, I.C., Eastham, S.D., Monier, E., Barrett, S.R.H., 2020. Premature mortality related to United States cross-state air pollution. *Nature* 578. <https://doi.org/10.1038/s41586-020-1983-8>
- Degraeuwe, B., Weiss, M., 2017. Does the New European Driving Cycle (NEDC) really fail to capture the NO X emissions of diesel cars in Europe ? *. *Environ. Pollut.* 222, 234–241. <https://doi.org/10.1016/j.envpol.2016.12.050>
- Deng, W., Fang, Z., Wang, Z., Zhu, M., Zhang, Y., Tang, M., Song, W., 2020. Primary emissions and secondary organic aerosol formation from in-use diesel vehicle exhaust : Comparison between idling and cruise mode. *Sci. Total Environ.* 699, 134357. <https://doi.org/10.1016/j.scitotenv.2019.134357>
- Deville Cavellin, L., Weichenthal, S., Tack, R., Ragettli, M.S., Smargiassi, A., Hatzopoulou, M., 2016. Investigating the Use Of Portable Air Pollution Sensors to Capture the Spatial Variability Of Traffic-Related Air Pollution. *Environ. Sci. Technol.* 50, 313–320. <https://doi.org/10.1021/acs.est.5b04235>
- Doherty, S.T., Lee-Gosselin, M., Papinski, D., 2006. An Internet-based Prompted Recall Diary with Automated GPS Activity-trip Detection: System Design. *Transp. Res. Board Annu. Meet.* 2005, 1–23.
- Esposito, E., De Vito, S., Salvato, M., Bright, V., Jones, R.L., Popoola, O., 2016. Dynamic neural network architectures for on field stochastic calibration of indicative low cost air quality sensing systems. *Sensors Actuators, B Chem.* 231, 701–713. <https://doi.org/10.1016/j.snb.2016.03.038>

- Evans, G., Audette, C., Badali, K., Celo, V., Dabek-Zlotorszynka, E., Debosz, J., Ding, L., Doerksen, G.N., Healy, R.M., Henderson, D., Herod, D., Hilker, N., Jeong, C.-H., Johnson, D., Jones, K., Munoz, A., Noble, M., Reid, K., Schiller, C., Sofowote, U., Su, Y., Wang, J., White, L., 2019. Near-Road Air Pollution Pilot Study Final Report.
- Fan, Y. Van, Perry, S., 2018. A review on air emissions assessment: Transportation 194. <https://doi.org/10.1016/j.jclepro.2018.05.151>
- Favez, J., Weilenmann, M., Stilli, J., 2009. Cold start extra emissions as a function of engine stop time: Evolution over the last 10 years. Atmos. Environ. 43, 996–1007. <https://doi.org/10.1016/j.atmosenv.2008.03.037>
- Franco, V., Kousoulidou, M., Muntean, M., Ntziachristos, L., Hausberger, S., Dilara, P., 2013. Road vehicle emission factors development: A review. Atmos. Environ. 70, 84–97. <https://doi.org/10.1016/j.atmosenv.2013.01.006>
- Gerard, D., Lave, L.B., 2005. Implementing technology-forcing policies: The 1970 Clean Air Act Amendments and the introduction of advanced automotive emissions controls in the United States. Technol. Forecast. Soc. Change 72, 761–778. <https://doi.org/10.1016/j.techfore.2004.08.003>
- Gertler, A.W., 2005. Diesel vs. gasoline emissions: Does PM from diesel or gasoline vehicles dominate in the US? Atmos. Environ. 39, 2349–2355. <https://doi.org/10.1016/j.atmosenv.2004.05.065>
- Gong, H., Zou, Y., Yang, Q., Fan, J., Sun, F., 2018. Generation of a driving cycle for battery electric vehicles: A case study of Beijing. Energy 150, 901–912. <https://doi.org/10.1016/j.energy.2018.02.092>
- Hasan, A.O., Elghawi, U.M., Al-muhtaseb, A.H., Abu-jrai, A., Al-rawashdeh, H., Tsolakis, A.,

2018. Influence of composite after-treatment catalyst on particle-bound polycyclic aromatic hydrocarbons – vapor-phase emitted from modern advanced GDI engines. *Fuel* 222, 424–433. <https://doi.org/10.1016/j.fuel.2018.02.114>
- He, L., Hu, J., Zhang, S., Wu, Y., Zhu, R., Zu, L., Bao, X., Lai, Y., Su, S., 2018. The impact from the direct injection and multi-port fuel injection technologies for gasoline vehicles on solid particle number and black carbon emissions. *Appl. Energy* 226, 819–826. <https://doi.org/10.1016/j.apenergy.2018.06.050>
- Health Canada, 2016. Human Health Risk Assessment for Diesel Exhaust.
- Henneman, L.R.F., Liu, C., Mulholland, J.A., Russell, A.G., Henneman, L.R.F., Liu, C., Mulholland, J.A., Armistead, G., 2017. Evaluating the effectiveness of air quality regulations : A review of accountability studies and frameworks. *J. Air Waste Manage. Assoc.* 67, 144–172. <https://doi.org/10.1080/10962247.2016.1242518>
- Hilker, N., Wang, J.M., Jeong, C.H., Healy, R.M., Sofowote, U., Debosz, J., Su, Y., Noble, M., Munoz, A., Doerksen, G., White, L., Audette, C., Herod, D., Brook, J.R., Evans, G.J., 2019. Traffic-related air pollution near roadways: Discerning local impacts from background. *Atmos. Meas. Tech.* 12, 5247–5261. <https://doi.org/10.5194/amt-12-5247-2019>
- Hodgson, A.W.E., Jacquinet, P., Hauser, P.C., 1999. Electrochemical Sensor for the Detection of SO₂ in the Low-ppb Range 71, 2831–2837. <https://doi.org/10.1021/ac9812429>
- Hossain, M., Sa, J., Baron, R., 2016. Differentiating NO₂ and O₃ at Low Cost Air Quality Amperometric Gas Sensors 2–5. <https://doi.org/10.1021/acssensors.6b00603>
- Huang, X., Wang, Y., Xing, Z., Du, K., 2016. Emission factors of air pollutants from CNG-gasoline bi-fuel vehicles: Part II. CO, HC and NO_x. *Sci. Total Environ.* 565, 698–705. <https://doi.org/10.1016/j.scitotenv.2016.05.069>

- Huang, Y., Organ, B., Zhou, J.L., Surawski, N.C., Hong, G., Chan, E.F.C., Yam, Y.S., 2018. Remote sensing of on-road vehicle emissions: Mechanism, applications and a case study from Hong Kong, in: *Atmospheric Environment*. Elsevier, pp. 58–74. <https://doi.org/10.1016/j.atmosenv.2018.03.035>
- Hudda, N., Fruin, S., Delfino, R.J., Sioutas, C., 2013. Efficient determination of vehicle emission factors by fuel use category using on-road measurements: downward trends on Los Angeles freight corridor I-710. *Atmos. Chem. Phys.* 13, 347–357. <https://doi.org/10.5194/acp-13-347-2013>
- Jabali, O., Laporte, G., 2016. A comparison of three idling options in long-haul truck scheduling 93, 631–647. <https://doi.org/10.1016/j.trb.2016.08.006>
- Jang, J., Lee, J., Kim, J., Park, S., 2015. Comparisons of the nanoparticle emission characteristics between GDI and PFI vehicles. *J. Nanoparticle Res.* 17, 1–14. <https://doi.org/10.1007/s11051-015-3280-2>
- Jiao, W., Hagler, G., Williams, R., Sharpe, R., Brown, R., Garver, D., Judge, R., Caudill, M., Rickard, J., Davis, M., Weinstock, L., Zimmer-Dauphinee, S., Buckley, K., 2016. Community Air Sensor Network (CAIRSENSE) project: Evaluation of low-cost sensor performance in a suburban environment in the southeastern United States. *Atmos. Meas. Tech.* 9, 5281–5292. <https://doi.org/10.5194/amt-9-5281-2016>
- Johnson, T., Joshi, A., 2017. Review of Vehicle Engine Efficiency and Emissions, in: *SAE Technical Papers*. pp. 1–23. <https://doi.org/10.4271/2017-01-0907>
- Karner, A.A., Eisinger, D.S., Niemeier, D.A., 2010. Near-Roadway Air Quality: Synthesizing the Findings from Real-World Data. *Environ. Sci. Technol.* 44, 5334–5344. <https://doi.org/10.1021/es100008x>

- Ke, H., Ondov, J.M., Rogge, W.F., 2013. Detailed emission profiles for on-road vehicles derived from ambient measurements during a windless traffic episode in Baltimore using a multi-model approach. *Atmos. Environ.* 81, 280–287. <https://doi.org/10.1016/j.atmosenv.2013.08.020>
- Kelly, F.J., Zhu, T., 2016. Transport solutions for cleaner air 352, 934–937.
- Kelly, K.E., Whitaker, J., Petty, A., Widmer, C., Dybwad, A., Sleeth, D., Martin, R., Butterfield, A., 2017. Ambient and laboratory evaluation of a low-cost particulate matter sensor. *Environ. Pollut.* 221, 491–500. <https://doi.org/10.1016/J.ENVPOL.2016.12.039>
- Kennedy, I.M., 2007. The health effects of combustion-generated aerosols. *Proc. Combust. Inst.* 31 II, 2757–2770. <https://doi.org/10.1016/j.proci.2006.08.116>
- Khan, T., Frey, H.C., 2018. Science of the Total Environment Comparison of real-world and certification emission rates for light duty gasoline vehicles. *Sci. Total Environ.* 622–623, 790–800. <https://doi.org/10.1016/j.scitotenv.2017.10.286>
- Ko, J., Jin, D., Jang, W., Myung, C., Kwon, S., Park, S., 2017. Comparative investigation of NO_x emission characteristics from a Euro 6-compliant diesel passenger car over the NEDC and WLTC at various ambient temperatures. *Appl. Energy* 187, 652–662. <https://doi.org/10.1016/j.apenergy.2016.11.105>
- Krecl, P., Targino, A.C., Landi, T.P., Ketznel, M., 2018. Determination of black carbon, PM_{2.5}, particle number and NO_x emission factors from roadside measurements and their implications for emission inventory development. *Atmos. Environ.* 186, 229–240. <https://doi.org/10.1016/j.atmosenv.2018.05.042>
- Kuklinska, K., Wolska, L., Namiesnik, J., Kuklinska, K., 2015. spheric Pollution. *Atmos. Pollut. Res.* 6, 129–137. <https://doi.org/10.5094/APR.2015.015>

- Kukutschová, J., Filip, P., 2018. Review of Brake Wear Emissions. <https://doi.org/10.1016/B978-0-12-811770-5.00006-6>
- Kumar, P., Morawska, L., Martani, C., Biskos, G., Neophytou, M., Di Sabatino, S., Bell, M., Norford, L., Britter, R., 2015. The rise of low-cost sensing for managing air pollution in cities. *Environ. Int.* 75, 199–205. <https://doi.org/10.1016/j.envint.2014.11.019>
- Kumar Pathak, S., Sood, V., Singh, Y., Channiwala, S.A., 2016. Real world vehicle emissions: Their correlation with driving parameters. *Transp. Res. Part D Transp. Environ.* 44, 157–176. <https://doi.org/10.1016/j.trd.2016.02.001>
- Larson, T., Gould, T., Riley, E.A., Austin, E., Fintzi, J., Sheppard, L., Yost, M., Simpson, C., 2017. Ambient air quality measurements from a continuously moving mobile platform : Estimation of area-wide , fuel-based , mobile source emission factors using absolute principal component scores. *Atmos. Environ.* 152, 201–211. <https://doi.org/10.1016/j.atmosenv.2016.12.037>
- Lawrence, S., Sokhi, R., Ravindra, K., 2016. Quantification of vehicle fleet PM10 particulate matter emission factors from exhaust and non-exhaust sources using tunnel measurement techniques. *Environ. Pollut.* 210, 419–428. <https://doi.org/10.1016/j.envpol.2016.01.011>
- Lee, Y., Lin, S., Yuan, C., Lin, M., Lin, S., Yuan, C., Lin, M., 2018. Reduction of atmospheric fine particle level by restricting the idling vehicles around a sensitive area. *J. Air Waste Manage. Assoc.* 68, 656–670. <https://doi.org/10.1080/10962247.2018.1438320>
- Leitl, B., Schatzmann, M., 2000. Physical modeling of emissions from naturally ventilated underground parking garages. *Environ. Monit. Assess.* 65, 221–229. <https://doi.org/10.1023/A:1006408411557>
- Lelieveld, J., Evans, J.S., Fnais, M., Giannadaki, D., Pozzer, A., 2015. The contribution of outdoor

- air pollution sources to premature mortality on a global scale. *Nature* 525, 367–371.
- Lewis, A.C., Lee, J.D., Edwards, P.M., Shaw, M.D., Evans, M.J., Moller, S.J., Smith, K.R., Buckley, J.W., Ellis, M., Gillot, S.R., White, A., 2016. Evaluating the performance of low cost chemical sensors for air pollution research. *Faraday Discuss.* 189, 85–103. <https://doi.org/10.1039/C5FD00201J>
- Li, H.Z., Gu, P., Ye, Q., Zimmerman, N., Robinson, E.S., Subramanian, R., Apte, J.S., Robinson, A.L., Presto, A.A., 2019. Spatially dense air pollutant sampling: Implications of spatial variability on the representativeness of stationary air pollutant monitors. *Atmos. Environ. X* 2, 100012. <https://doi.org/10.1016/j.aeaoa.2019.100012>
- Li, X., Dallmann, T.R., May, A.A., Presto, A.A., 2020. Seasonal and long-term trend of on-road gasoline and diesel vehicle emission factors measured in traffic tunnels. *Appl. Sci.* 10. <https://doi.org/10.3390/app10072458>
- Li, X., Dallmann, T.R., May, A.A., Stanier, C.O., Grieshop, A.P., Lipsky, E.M., Robinson, A.L., Presto, A.A., 2018. Size distribution of vehicle emitted primary particles measured in a traffic tunnel. *Atmos. Environ.* 191, 9–18. <https://doi.org/10.1016/j.atmosenv.2018.07.052>
- Ligterink, N.E., 2016. Emissions of three common GDI vehicles Emissions of three common GDI vehicles. <https://doi.org/10.13140/RG.2.2.19876.68489>
- Lin, C., Gong, B., Qu, X., 2015. Low emissions and delay optimization for an isolated signalized intersection based on vehicular trajectories. *PLoS One* 10, 1–17. <https://doi.org/10.1371/journal.pone.0146018>
- Lu, W.Z., He, H. Di, Dong, L. yun, 2011. Performance assessment of air quality monitoring networks using principal component analysis and cluster analysis. *Build. Environ.* 46, 577–583. <https://doi.org/10.1016/j.buildenv.2010.09.004>

- Maag, B., Zhou, Z., Thiele, L., 2018. A Survey on Sensor Calibration in Air Pollution Monitoring Deployments 5, 4857–4870.
- Malings, C., Tanzer, R., Hauryliuk, A., Kumar, S.P.N., Zimmerman, N., Kara, L.B., Presto, A.A., Subramanian, R., 2019. Development of a general calibration model and long-term performance evaluation of low-cost sensors for air pollutant gas monitoring. *Atmos. Meas. Tech.* 12, 903–920. <https://doi.org/10.5194/amt-12-903-2019>
- Malings, C., Tanzer, R., Hauryliuk, A., Saha, P.K., Allen, L., Presto, A.A., Subramanian, R., Malings, C., Tanzer, R., Hauryliuk, A., Saha, P.K., Allen, L., Ñ, C.M., Tanzer, R., Hauryliuk, A., Saha, P.K., Robinson, A.L., Presto, A.A., Subramanian, R., 2020. Fine particle mass monitoring with low-cost sensors : Corrections and long-term performance evaluation term performance evaluation. *Aerosol Sci. Technol.* 54, 160–174. <https://doi.org/10.1080/02786826.2019.1623863>
- Man, H., Liu, H., Xiao, Q., Deng, F., Yu, Q., Wang, K., Yang, Z., Wu, Y., He, K., Hao, J., 2020. How ethanol and gasoline formula changes evaporative emissions of the vehicles 222, 584–594. <https://doi.org/10.1016/j.apenergy.2018.03.109>
- Masson, N., Piedrahita, R., Hannigan, M., 2015. Approach for quantification of metal oxide type semiconductor gas sensors used for ambient air quality monitoring. *Sensors Actuators, B Chem.* 208, 339–345. <https://doi.org/10.1016/j.snb.2014.11.032>
- May, A.A., Nguyen, N.T., Presto, A.A., Gordon, T.D., Lipsky, E.M., Karve, M., Gutierrez, A., Robertson, W.H., Zhang, M., Brandow, C., Chang, O., Chen, S., Cicero-Fernandez, P., Dinkins, L., Fuentes, M., Huang, S.-M., Ling, R., Long, J., Maddox, C., Massetti, J., McCauley, E., Miguel, A., Na, K., Ong, R., Pang, Y., Rieger, P., Sax, T., Truong, T., Vo, T., Chattopadhyay, S., Maldonado, H., Maricq, M.M., Robinson, A.L., 2014. Gas- and particle-

- phase primary emissions from in-use, on-road gasoline and diesel vehicles. *Atmos. Environ.* 88, 247–260. <https://doi.org/10.1016/j.atmosenv.2014.01.046>
- May, X., Basu, R., Malig, B., Broadwin, R., Ebisu, K., Gold, E.B., Qi, L., Derby, C., Green, R.S., 2017. Association between gaseous air pollutants and inflammatory, hemostatic and lipid markers in a cohort of midlife women. *Environ. Int.* 107, 131–139. <https://doi.org/10.1016/j.envint.2017.07.004>
- Mead, M.I., Popoola, O.A.M., Stewart, G.B., Landshoff, P., Calleja, M., Hayes, M., Baldovi, J.J., McLeod, M.W., Hodgson, T.F., Dicks, J., Lewis, A., Cohen, J., Baron, R., Saffell, J.R., Jones, R.L., 2013. The use of electrochemical sensors for monitoring urban air quality in low-cost, high-density networks. *Atmos. Environ.* 70, 186–203. <https://doi.org/10.1016/j.atmosenv.2012.11.060>
- Meng, J., Martin, R. V, Li, C., Van Donkelaar, A., Tzompa-Sosa, Z.A., Yue, X., Xu, J.W., Weagle, C.L., Burnett, R.T., 2019. Source Contributions to Ambient Fine Particulate Matter for Canada. *Environ. Sci. Technol.* 53, 10269–10278. <https://doi.org/10.1021/acs.est.9b02461>
- Moltchanov, S., Levy, I., Etzion, Y., Lerner, U., Broday, D.M., Fishbain, B., 2015. On the feasibility of measuring urban air pollution by wireless distributed sensor networks. *Sci. Total Environ.* 502, 537–547. <https://doi.org/10.1016/j.scitotenv.2014.09.059>
- Nam, E.K., Mitcham, A., 2019. Dynamometer and On-board Emissions Testing of the Honda Insight and Toyota Prius 2005.
- Pang, X., Shaw, M.D., Gillot, S., Lewis, A.C., 2018. Chemical The impacts of water vapour and co-pollutants on the performance of electrochemical gas sensors used for air quality monitoring. *Sensors Actuators B. Chem.* 266, 674–684. <https://doi.org/10.1016/j.snb.2018.03.144>

- Papapostolou, V., Zhang, H., Feenstra, B.J., Polidori, A., 2017. Development of an environmental chamber for evaluating the performance of low-cost air quality sensors under controlled conditions. *Atmos. Environ.* 171, 82–90. <https://doi.org/10.1016/j.atmosenv.2017.10.003>
- Pereira, G., Bell, M.L., Lee, H.J., Koutrakis, P., Belanger, K., 2014. Research | Children ' s Health Sources of Fine Particulate Matter and Risk of Preterm Birth in Connecticut , 122, 1117–1122.
- Peters, S., Klerk, N. De, Reid, A., Fritsch, L., Musk, A.W.B., Vermeulen, R., 2017. Estimation of quantitative levels of diesel exhaust exposure and the health impact in the contemporary Australian mining industry 282–289. <https://doi.org/10.1136/oemed-2016-103808>
- Pokharel, S.S., Bishop, G.A., Stedman, D.H., 2002. An on-road motor vehicle emissions inventory for Denver: An efficient alternative to modeling. *Atmos. Environ.* 36, 5177–5184. [https://doi.org/10.1016/S1352-2310\(02\)00651-9](https://doi.org/10.1016/S1352-2310(02)00651-9)
- Qiao, F., Yu, L., Vojtisek-Lom, M., 2005. On-road vehicle emission and activity data collection and evaluation in Houston, Texas, in: *Transportation Research Record*. pp. 60–71. <https://doi.org/10.3141/1941-08>
- Quiros, D.C., Smith, J.D., Ham, W.A., Robertson, W.H., Ayala, A., Hu, S., Quiros, D.C., Smith, J.D., Ham, W.A., Robertson, W.H., Quiros, D.C., Smith, J.D., Ham, W.A., Robertson, W.H., Huai, T., Ayala, A., 2018. Deriving fuel-based emission factor thresholds to interpret heavy-duty vehicle roadside plume measurements roadside plume measurements. *J. Air Waste Manage. Assoc.* 68, 969–987. <https://doi.org/10.1080/10962247.2018.1460637>
- Rakha, H., Van Aerde, M., Ahn, K., Trani, a. a., 2000. Requirements for evaluating traffic signal control impacts on energy and emissions based on instantaneous speed and acceleration measurements. *Transp. Res. Rec.* 56–67. <https://doi.org/10.3141/1738-07>

- Ramos, A., Muñoz, J., Andrés, F., Armas, O., 2018. NO_x emissions from diesel light duty vehicle tested under NEDC and real-world driving conditions. *Transp. Res. Part D* 63, 37–48. <https://doi.org/10.1016/j.trd.2018.04.018>
- Reiter, M.S., Kockelman, K.M., 2016. The problem of cold starts : A closer look at mobile source emissions levels. *Transp. Res. Part D* 43, 123–132. <https://doi.org/10.1016/j.trd.2015.12.012>
- Rice, M.B., Rifas-Shiman, S.L., Litonjua, A.A., Oken, E., Gillman, M.W., Kloog, I., Luttmann-Gibson, H., Zanobetti, A., Coull, B.A., Schwartz, J., Koutrakis, P., Mittleman, M.A., Gold, D.R., 2016. Lifetime exposure to ambient pollution and lung function in children. *Am. J. Respir. Crit. Care Med.* 193, 881–888. <https://doi.org/10.1164/rccm.201506-1058OC>
- Ropkins, K., DeFries, T.H., Pope, F., Green, D.C., Kemper, J., Kishan, S., Fuller, G.W., Li, H., Sidebottom, J., Crilley, L.R., Kramer, L., Bloss, W.J., Stewart Hager, J., 2017. Evaluation of EDAR vehicle emissions remote sensing technology. *Sci. Total Environ.* 609, 1464–1474. <https://doi.org/10.1016/j.scitotenv.2017.07.137>
- Silverman, D.T., 2012. Diesel exhaust causes lung cancer : now what ? 233–234. <https://doi.org/10.1136/oemed-2016-104197>
- Singer, B.C., Kirchstetter, T.W., Harley, R.A., Kendall, G.R., Hesson, J.M., 1999. A fuel-based approach to estimating motor vehicle cold-start emissions. *J. Air Waste Manag. Assoc.* 49, 125–135. <https://doi.org/10.1080/10473289.1999.10463785>
- Snyder, E.G., Watkins, T.H., Solomon, P.A., Thoma, E.D., Williams, R.W., Hagler, G.S.W., Shelow, D., Hindin, D.A., Kilaru, V.J., Preuss, P.W., 2013. The changing paradigm of air pollution monitoring. *Environ. Sci. Technol.* 47, 11369–11377. <https://doi.org/10.1021/es4022602>
- Start, C., Of, E., Low, A.T., Temperatures, A., An, A.S., Quality, A.I.R., 2014. AT LOW

<https://doi.org/10.2478/aep-2014-0026>

Stern, A.C., Stern, A.C., Hill, C., Carolina, N., 2012. History of Air Pollution Legislation in the United States 2470. <https://doi.org/10.1080/00022470.1982.10465369>

Suarez-bertoa, R., Astorga, C., 2018. Impact of cold temperature on Euro 6 passenger car emissions *. *Environ. Pollut.* 234, 318–329. <https://doi.org/10.1016/j.envpol.2017.10.096>

Taxell, P., Santonen, T., 2017. Diesel Engine Exhaust : Basis for Occupational Exposure Limit Value 158, 243–251. <https://doi.org/10.1093/toxsci/kfx110>

Thomas, D., Li, H., Ropkins, K., Wang, X., Ge, Y., 2020. Investigating the engine behavior of a hybrid vehicle and its impact on regulated emissions during on-road testing.

Thurnheer, T., Edenhauser, D., Soltic, P., Schreiber, D., Kirchen, P., Sankowski, A., 2011. Experimental investigation on different injection strategies in a heavy-duty diesel engine : Emissions and loss analysis. *Energy Convers. Manag.* 52, 457–467. <https://doi.org/10.1016/j.enconman.2010.06.074>

Tietge, U., Zacharof, N., Mock, P., Franco, V., German, J., Bandivadekar, A., Ligterink, N., Lambrecht, U., 2015a. From laboratory to road: A 2015 update of official And “real-world” fuel consumption And CO₂ values for passenger cars in Europe, ICCT White Papers.

Tietge, U., Zacharof, N., Mock, P., Franco, V., German, J., Icct, A.B., Tno, N.L., Ifeu, U.L., 2015b. FROM LABORATORY TO ROAD.

Tsokolis, D., Tsiakmakis, S., Dimaratos, A., Fontaras, G., Pistikopoulos, P., Ciuffo, B., Samaras, Z., 2020. Fuel consumption and CO₂ emissions of passenger cars over the New Worldwide Harmonized Test Protocol q. *Appl. Energy* 179, 1152–1165. <https://doi.org/10.1016/j.apenergy.2016.07.091>

- U.S. Department of Energy, 2020. Annual Energy Outlook 2020.
- U.S. Environmental Protection Agency, 2016. Monitoring PM_{2.5} in Ambient Air Using Designated Reference or Class I Equivalent Methods.
- USEPA, 2016. Quality Assurance Guidance Document 2.12: Monitoring PM_{2.5} in Ambient Air Using Designated Reference or Class 1 Equivalent Methods 174. <https://doi.org/EPA-454/B-16-001>
- Vlachos, T.G., Bonnel, P., Perujo, A., Weiss, M., Villafuerte, P.M., Riccobono, F., 2019. In-Use Emissions Testing with Portable Emissions Measurement Systems (PEMS) in the Current and Future European Vehicle Emissions Legislation : Overview , Underlying Principles and Expected Benefits. <https://doi.org/10.4271/2014-01-1549>
- Wang, C., Xu, H., Herreros, J.M., Wang, J., Cracknell, R., 2014. Impact of fuel and injection system on particle emissions from a GDI engine. *Appl. Energy* 132, 178–191. <https://doi.org/10.1016/j.apenergy.2014.06.012>
- Wang, H., Chen, C., Huang, C., Fu, L., 2008. On-road vehicle emission inventory and its uncertainty analysis for Shanghai, China. *Sci. Total Environ.* 398, 60–67. <https://doi.org/10.1016/j.scitotenv.2008.01.038>
- Wang, J.M., Jeong, C.H., Hilker, N., Shairsingh, K.K., Healy, R.M., Sofowote, U., Deboasz, J., Su, Y., McGaughey, M., Doerksen, G., Munoz, T., White, L., Herod, D., Evans, G.J., 2018a. Near-Road Air Pollutant Measurements: Accounting for Inter-Site Variability Using Emission Factors. *Environ. Sci. Technol.* 52, 9495–9504. <https://doi.org/10.1021/acs.est.8b01914>
- Wang, J.M., Jeong, C.H., Zimmerman, N., Healy, R.M., Evans, G.J., 2018b. Real world vehicle fleet emission factors: Seasonal and diurnal variations in traffic related air pollutants. *Atmos.*

- Environ. 184, 77–86. <https://doi.org/10.1016/j.atmosenv.2018.04.015>
- Wang, J.M., Jeong, C.H., Zimmerman, N., Healy, R.M., Wang, D.K., Ke, F., Evans, G.J., 2015. Plume-based analysis of vehicle fleet air pollutant emissions and the contribution from high emitters. *Atmos. Meas. Tech.* 8, 3263–3275. <https://doi.org/10.5194/amt-8-3263-2015>
- Wang, Q., Huo, H., He, K., Yao, Z., Zhang, Q., 2008. Characterization of vehicle driving patterns and development of driving cycles in Chinese cities 13, 289–297. <https://doi.org/10.1016/j.trd.2008.03.003>
- Wong, G.W.K., 2014. Air pollution and health. *Lancet Respir. Med.* [https://doi.org/10.1016/S2213-2600\(13\)70284-4](https://doi.org/10.1016/S2213-2600(13)70284-4)
- Wu, S., Ni, Y., Li, H., Pan, L., Yang, D., Baccarelli, A.A., Deng, F., Chen, Y., Shima, M., Guo, X., 2016. Short-term exposure to high ambient air pollution increases airway inflammation and respiratory symptoms in chronic obstructive pulmonary disease patients in Beijing, China. *Environ. Int.* 94, 76–82. <https://doi.org/10.1016/j.envint.2016.05.004>
- Yamada, H., Inomata, S., Tanimoto, H., Hata, H., Tonokura, K., 2018. Science of the Total Environment Estimation of refueling emissions based on theoretical model and effects of E10 fuel on refueling and evaporative emissions from gasoline cars. *Sci. Total Environ.* 622–623, 467–473. <https://doi.org/10.1016/j.scitotenv.2017.11.339>
- Yang, B., Soc, J.E., Yang, B., Wang, C., Xiao, R., Yu, H., Wang, J., Xu, J., Liu, H., Xia, F., Xiao, J., 2019. CO Response Characteristics of NiFe₂O₄ Sensing Material at Elevated Temperature CO Response Characteristics of NiFe₂O₄ Sensing Material at Elevated Temperature 2–7. <https://doi.org/10.1149/2.0581912jes>
- Yao, Y., Tsai, J., Ye, H., Chiang, H., Yao, Y., Tsai, J., Ye, H., 2012. Comparison of Exhaust Emissions Resulting from Cold- and Hot-Start Motorcycle Driving Modes Comparison of

Exhaust Emissions Resulting from Cold- and Hot-Start Motorcycle Driving Modes 2247.
<https://doi.org/10.3155/1047-3289.59.11.1339>

Yao, Y.C., Tsai, J.H., Ye, H.F., Chiang, H.L., 2009. Comparison of exhaust emissions resulting from cold- and hot-start motorcycle driving modes. *J. Air Waste Manag. Assoc.* 59, 1339–1346. <https://doi.org/10.3155/1047-3289.59.11.1339>

Yli-Tuomi, T., Aarnio, P., Pirjola, L., Mäkelä, T., Hillamo, R., Jantunen, M., 2005. Emissions of fine particles, NO_x, and CO from on-road vehicles in Finland. *Atmos. Environ.* 39, 6696–6706. <https://doi.org/10.1016/j.atmosenv.2005.07.049>

York, A., Rouleau, M., 2017. Can traffic management strategies improve urban air quality? A review of the evidence. *J. Transp. Heal.* 7, 111–124. <https://doi.org/10.1016/j.jth.2017.08.001>

Yuan, X., Li, L., Gou, H., Dong, T., 2015. Energy and environmental impact of battery electric vehicle range in China. *Appl. Energy* 157, 75–84. <https://doi.org/10.1016/j.apenergy.2015.08.001>

Zhang, Y., Deng, W., Hu, Q., Wu, Z., Yang, W., Zhang, H., Wang, Z., 2020. Comparison between idling and cruising gasoline vehicles in primary emissions and secondary organic aerosol formation during photochemical ageing. *Sci. Total Environ.* 722, 137934. <https://doi.org/10.1016/j.scitotenv.2020.137934>

Zhao, F., Lai, M.C., Harrington, D.L., 1999. Automotive spark-ignited direct-injection gasoline engines. *Prog. Energy Combust. Sci.* 25, 437–562. [https://doi.org/10.1016/S0360-1285\(99\)00004-0](https://doi.org/10.1016/S0360-1285(99)00004-0)

Zhu, R., Hu, J., Bao, X., He, L., Lai, Y., Zu, L., Li, Y., Su, S., 2016. Tailpipe emissions from gasoline direct injection (GDI) and port fuel injection (PFI) vehicles at both low and high ambient temperatures. *Environ. Pollut.* 216, 223–234.

<https://doi.org/10.1016/j.envpol.2016.05.066>

Zimmerman, N., 2016. Linking laboratory engine studies to real-world observations: Assessing the air quality implications of gasoline direct injection engines. University of Toronto: Toronto, Canada.

Zimmerman, N., Presto, A.A., Kumar, S.P.N., Gu, J., Hauryliuk, A., Robinson, E.S., Robinson, A.L., Subramanian, R., 2018. A machine learning calibration model using random forests to improve sensor performance for lower-cost air quality monitoring. *Atmos. Meas. Tech.* 11, 291–313. <https://doi.org/10.5194/amt-11-291-2018>

Zimmerman, N., Wang, J.M., Jeong, C.-H., Ramos, M., Hilker, N., Healy, R.M., Sabaliauskas, K., Wallace, J.S., Evans, G., 2016. Field measurements of gasoline direct injection emission factors: spatial and seasonal variability. *Environ. Sci. Technol.* 50, 2035–2043. <https://doi.org/10.1021/acs.est.5b04444>

Appendices

Appendix A

A.1 Plume detection and matching details.

Using the vehicle count data provided by Parking Services, we analyzed the average background subtracted concentrations between 1-4AM, removing periods when vehicles entered/exited the parking garages, and used this as a representative noise signal. Since the sensors can also be also influenced by vehicles passing by on the main road outside the parking garages, we took the 90th percentile value as the noise signal and to determine our plume threshold. The cut-off value for each pollutant is different between sensors and has been listed in Table A1.

	AG1 entrance	AG1 center	AG2 entrance	AG2 center	BG1 entrance	BG1 center
CO ₂ (ppm)	3.9	5.2	4.4	5.1	5.5	3.4
CO (ppb)	15	16	13	17	34	24
NO (ppb)	0.5	1.0	0.4	0.9	1.0	1.1
NO ₂ (ppb)	2.9	1.8	2.1	2.4	2.6	1.1
PM _{2.5} (µg/m ³)	0.8	0.7	0.7	0.6	0.7	0.5

Table A.1 Pollutant cut-off values at the different measurement sites to determine our plume threshold.

For a pollutant plume to be identified, it needed to be matched with a CO₂ plume also meeting the plume identification criteria. The number and percentage of matched plumes is provided in Table A.2.

	AG1 entrance	AG1 center	AG2 entrance	AG2 center	BG1 entrance	BG1 center	Total
CO ₂	95% (1431/1504)	92% (1970/2128)	94% (1271/1351)	94% (2609/2778)	70% (2060/2947)	89% (1714/1934)	87% (11055/12642)
CO	50% (1237/2479)	72% (1728/2404)	54% (1077/1975)	81% (2194/2698)	78% (1883/2401)	65% (1156/1766)	67% (9275/13723)
NO	47% (1223/2576)	74% (1721/2325)	49% (951/1945)	78% (2350/3000)	76% (1834/2398)	64% (1336/2097)	66% (9415/14341)
NO ₂	79% (638/806)	83% (1343/1620)	57% (1034/1802)	84% (1748/2070)	74% (1775/2386)	66% (1214/1826)	74% (7752/10510)
PM _{2.5}	28% (365/1306)	50% (331/660)	30% (158/525)	64% (962/1501)	49% (271/547)	39% (470/1214)	44% (2557/5753)

Table A.2 Number of matched pollutant-CO₂ plumes for emission factor calculations.

A.2 Diurnal trend of hourly average pollutant concentrations before and after background subtraction

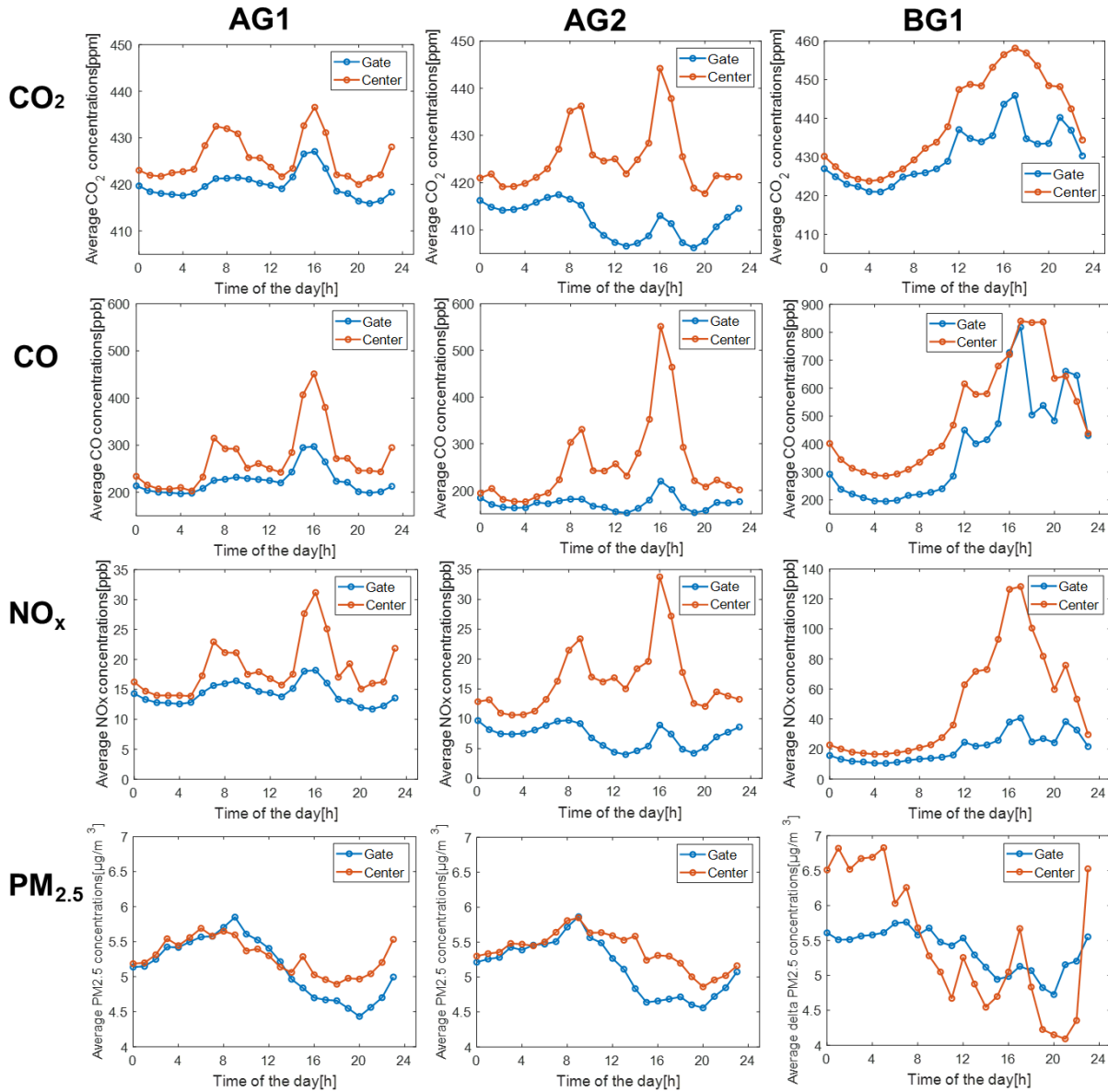


Figure A.1 Diurnal trends of hourly average pollutant total concentrations. The orange curve is the concentration at the center of the garage and the blue curve is the concentration at the gate of the garage.

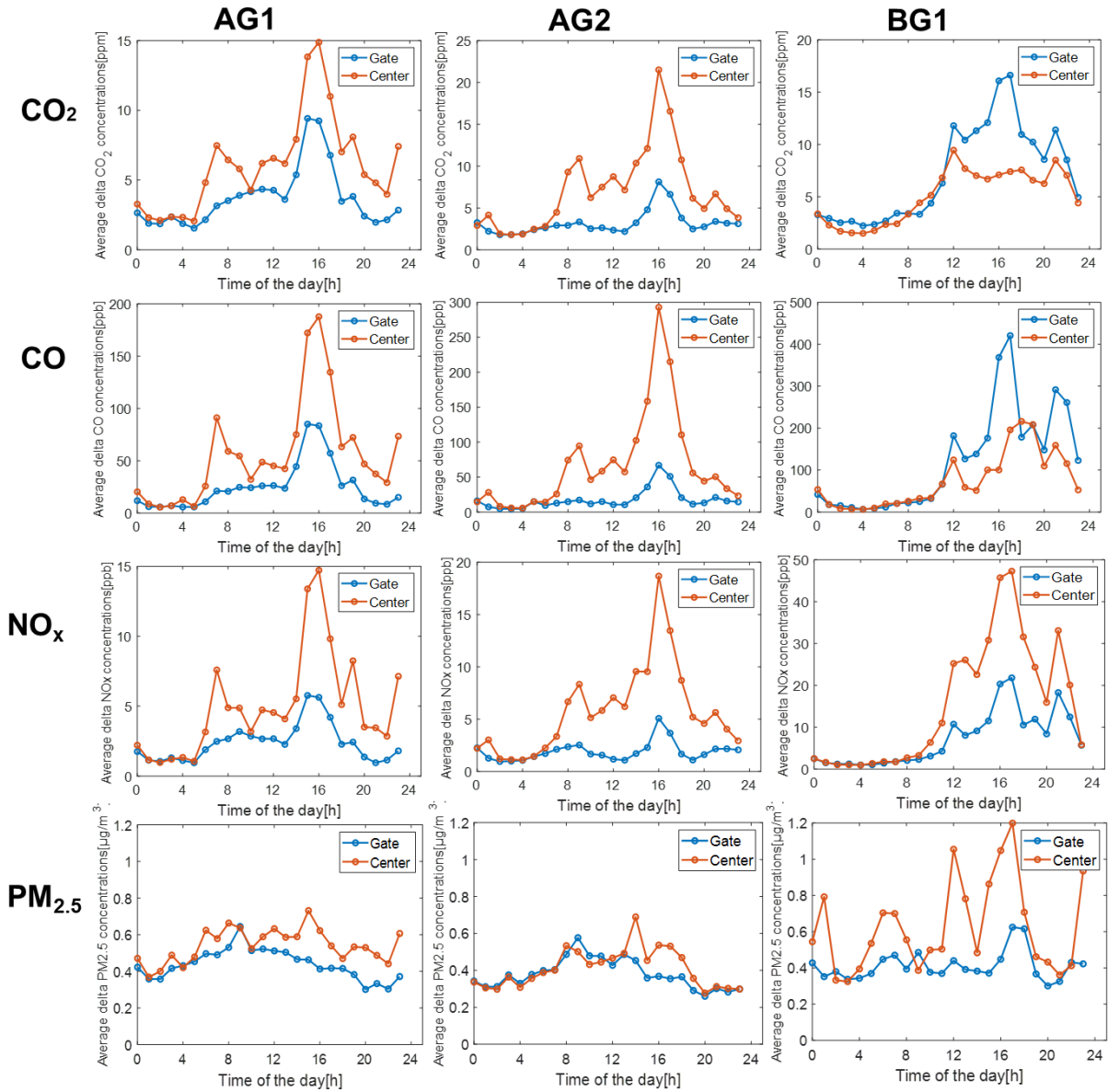


Figure A.2 Diurnal trends of hourly average background-subtracted concentrations. The orange curve is the concentration at the center of the garage and the blue curve is the concentration at the gate of the garage.